comptes rendus palevol

2022 • 21 • 20

A new late Eocene alligatoroid crocodyliform from Transylvania

Márton VENCZEL & Vlad A. CODREA

art. 21 (20) — Published on 17 May 2022
www.cr-palevol.fr

PUBLICATIONS SCIENTIFIQUES

Couverture / *Cover*:
Made from the Figures of the article.

Comptes Rendus Palevol est indexé dans / Comptes Rendus Palevol *is indexed by:*
– Cambridge Scientific Abstracts
– Current Contents® Physical
– Chemical, and Earth Sciences®
– ISI Alerting Services®
– Geoabstracts, Geobase, Georef, Inspec, Pascal
– Science Citation Index®, Science Citation Index Expanded®
– Scopus®.

Les articles ainsi que les nouveautés nomenclaturales publiés dans *Comptes Rendus Palevol* sont référencés par / *Articles and nomenclatural novelties published in* Comptes Rendus Palevol *are registered on:*
– ZooBank® (http://zoobank.org)

Comptes Rendus Palevol est une revue en flux continu publiée par les Publications scientifiques du Muséum, Paris et l'Académie des sciences, Paris
Comptes Rendus Palevol *is a fast track journal published by the Museum Science Press, Paris and the Académie des sciences, Paris*

Les Publications scientifiques du Muséum publient aussi / *The Museum Science Press also publish:*
Adansonia, ***Geodiversitas***, ***Zoosystema***, ***Anthropozoologica***, ***European Journal of Taxonomy***, ***Naturae***, ***Cryptogamie*** **sous-sections** ***Algologie***, ***Bryologie***, ***Mycologie***.

L'Académie des sciences publie aussi / *The Académie des sciences also publishes:*
Comptes Rendus Mathématique, ***Comptes Rendus Physique***, ***Comptes Rendus Mécanique***, ***Comptes Rendus Chimie***, ***Comptes Rendus Géoscience***, ***Comptes Rendus Biologies***.

Diffusion – Publications scientifiques Muséum national d'Histoire naturelle
CP 41 – 57 rue Cuvier F-75231 Paris cedex 05 (France)
Tél.: 33 (0)1 40 79 48 05 / Fax: 33 (0)1 40 79 38 40
diff.pub@mnhn.fr / https://sciencepress.mnhn.fr

Académie des sciences, Institut de France, 23 quai de Conti, 75006 Paris.

ISSN (imprimé / *print*): 1631-0683/ ISSN (électronique / *electronic*): 1777-571X

A new late Eocene alligatoroid crocodyliform from Transylvania

Márton VENCZEL
Țării Crișurilor Museum, 1/A Armatei Române Str. RO-410087, Oradea (Romania)
and Babeș-Bolyai University, Laboratory of Palaeotheriology and Quaternary Geology, Department of Geology-Palaeontology, 1 Kogălniceanu Str. RO-400084, Cluj-Napoca (Romania)

Vlad A. CODREA
Babeș-Bolyai University, Laboratory of Palaeotheriology and Quaternary Geology, Department of Geology-Palaeontology, 1 Kogălniceanu Str. RO-400084, Cluj-Napoca (Romania)
codrea_vlad@yahoo.fr (corresponding author)

Submitted on 10 October 2020 | Accepted on 22 January 2021 | Published on 17 May 2022

urn:lsid:zoobank.org:pub:62258E37-8548-4DC8-8E97-177F8EEF99B0

Venczel M. & Codrea V. A. 2022. — A new late Eocene alligatoroid crocodyliform from Transylvania. *Comptes Rendus Palevol* 21 (20): 411-429. https://doi.org/10.5852/cr-palevol2022v21a20

ABSTRACT
Here we describe a new eusuchian crocodyliform, collected 130 years ago from a shallow marine limestone of the late Eocene (Priabonian) fossil locality of Cluj-Mănăștur, Transylvania, Romania. *Diplocynodon kochi* n. sp. is represented by a three-dimensionally preserved incomplete skull that may have belonged to a mature individual. The new taxon possesses a relatively narrow and elongated snout and a mediolaterally shallow but anteroposteriorly wide premaxillary-maxillary notch, strengthened by a prominent bony ridge. The nasals are excluded from the naris and the anterior tip of the frontal forms a broad, complex sutural contact with the nasals. *Diplocynodon kochi* n. sp. possesses, similarly to other members of the genus, 16-17 maxillary alveoli of which the fourth and fifth alveoli are enlarged and confluent; the lacrimal is longer than the prefrontal; the ectopterygoid is situated close to the posteriormost maxillary tooth alveoli, the dorsal margin of the infratemporal fenestra is bordered by the quadratojugal, preventing the quadrate from reaching the fenestra, and the foramen aëreum is situated on the dorsal surface of the quadrate. The occurrence of *D. kochi* n. sp. in the Priabonian of the eastern part of Central Europe suggests that the genus was still present and probably widespread across the continent that contributed probably to its survival (at least locally) across the Eocene/Oligocene boundary.

KEY WORDS
Carbonate platform, *Diplocynodon*, faunal diversity, paratethys, Priabonian, new species.

RÉSUMÉ
Un nouveau crocodyliforme alligatoroïde de l'Éocène supérieur de Transylvanie.
Nous décrivons ici un nouveau crocodyliforme eusuchien découvert il y a environ 130 ans dans un calcaire marin peu profond de la localité de Cluj-Mănăștur (Transylvanie, Roumanie), datant de l'Éocène supérieur (Priabonien). *Diplocynodon kochi* n. sp. est représenté par un crâne incomplet, préservé en trois dimensions, appartenant à un individu vraisemblablement mature. Le nouveau taxon possède un museau de type platyrostre, relativement étroit et allongé et une encoche prémaxillaire-maxillaire médio-latéralement peu profonde, mais antéropostérieurement longue, renforcée par une

crête osseuse proéminente. L'os nasal est exclu des narines et l'extrémité antérieure du frontal forme un contact sutural grand et complexe avec l'os nasal. *Diplocynodon kochi* n. sp. possède, comme les autres membres du genre, 16-17 alvéoles sur le maxillaire, dont les quatrième et cinquième alvéoles sont grands et confluents ; le lacrymal est plus long que le préfrontal ; l'ectoptérygoïde est positionné près des alvéoles des maxillaires les plus postérieures ; la marge dorsale de la fenêtre infra-temporale est bordée par le quadratojugal, séparant ainsi le carré de la fenêtre infratemporale ; et le foramen aëreum est situé sur la surface dorsale du carré. La présence de *D. kochi* dans le Priabonien de la partie orientale de l'Europe centrale suggère que le genre était encore présent et probablement largement distribué sur le continent, ce qui a probablement contribué à sa survie (au moins localement) au-delà de la limite Éocène/Oligocène.

MOTS CLÉS
Plateforme carbonatée,
Diplocynodon,
diversité faunique,
paratethys,
Priabonien,
espèce nouvelle.

INTRODUCTION

The Palaeocene-Eocene fossil record of European crocodyliforms revealed a moderately high diversity that included notosuchians, like *Bergisuchus* Kuhn, 1968 (Eocene of Germany) and *Iberosuchus* Antunes, 1975 (Eocene of France, Portugal and Spain) (Berg 1966; Kuhn 1968; Antunes 1975; Buffetaut 1988; Ortega *et al.* 1996; Rossmann 2000; Martin 2015, 2016), eusuchians represented by ziphodont planocraniids, like *Boverisuchus* Kuhn, 1938 (Eocene of France, Germany, Italy, Spain) (Brochu 2013), crocodyloids like *Asiatosuchus* Mook, 1940 (Palaeocene of France and Eocene of Germany) (Berg 1966; Delfino & Smith 2009; Delfino *et al.* 2017) and *Megadontosuchus arduini* de Zigno, 1880 (middle Eocene of Italy)(Piras *et al.* 2007), gavialoids like *Eosuchus* Dollo, 1907 (Palaeocene of France) (Delfino *et al.* 2005; Brochu 2007) and alligatoroids, like *Hassiacosuchus* Weitzel, 1935 (Eocene of Germany)(Brochu 2004) and *Diplocynodon* Pomel, 1847, the latter having a more extended fossil record from the Palaeocene up to the middle Miocene (Martin *et al.* 2014; Rio *et al.* 2020 and references therein). Close to the Eocene-Oligocene boundary, the deteriorating climatic conditions produced a drop in the diversity of crocodylian assemblages (Martin 2010), and as a consequence the only clade that survived the so called "Grande Coupure" (Stehlin 1909) was *Diplocynodon* (Antunes & Cahuzac 1999; Piras & Buscalioni 2006; Martin 2010; Čerňanský *et al.* 2012; Chroust *et al.* 2019; Luján *et al.* 2019; Macaluso *et al.* 2019). The fossil records of Palaeocene-Eocene crocodyliforms are mostly known from the western part of Europe and only a few fossils have been reported from the eastern part of the continent including Northwest Romania (Koch 1894; Codrea & Venczel 2020).

Here, we describe a specimen of *Diplocynodon* collected about 130 years ago (in 1890) from a former limestone quarry at Cluj-Mănăștur of late Eocene (Priabonian) age and subsequently reported by Koch (1894: 247) as resembling "*Crocodilus communis*". A single specimen was recovered from three samples of bioclastic limestone, probably shattered when collected, exposing an incomplete skull in ventral view that preserved the premaxillae, the maxillae, the anterior parts of the paired palatines, the quadrates, part of the left pterygoid with impressions of the secondary choanae and most of the left ectopterygoid. Probably, part of the skull was damaged at the time of collecting by quarry workers, the posterior part of the right maxilla being broken off and subsequently lost along with the slab enclosing the counterpart of the specimen that contained possibly the remaining parts of the palatines, the right pterygoid and the right ectopterygoid. Based on its preserved morphological features (e.g. the fourth and fifth maxillary alveoli are enlarged; the lacrimal is longer than the prefrontal; the dorsal margin of the infratemporal fenestra is formed by the quadratojugal, preventing the quadrate from reaching the fenestra; 16-17 maxillary alveoli are present), the specimen is included with confidence in the genus *Diplocynodon* (see Martin *et al.* 2014).

In the present paper we: 1) describe the skull of the new alligatoroid crocodyliform discovered in the Cluj-Mănăștur fossil locality and assign it, based on its combination of characters, to a new species of *Diplocynodon*; 2) test the phylogenetic relationships of the new taxon; and 3) discuss the taphonomic, palaeoenvironmental and palaeogeographic contexts of the discovered remains.

MATERIAL AND METHODS

The fossil material reported here consists of an incomplete three-dimensional skull. The skull was kept until present embedded in coarse limestone, broken into three pieces of rock, exposing the ventral side of the premaxilla, maxilla, palatine and parts and traces of the pterygoid and ectopterygoid (Fig. 1). The three parts of the specimen were prepared mechanically, strengthened and reunited using mowilith (Codrea & Venczel 2020). The specimen lacks any sign of abrasion on the dorsal surface of the skull that precludes a long-distance transport. However, some bones are missing from the left cranial part (most part of the prefrontal, squamosal and quadratojugal) exposing in part the articular surface between the quadrate and squamosal. Detachment of the above bones may have resulted from physical pressure of the accumulating gases or from other natural causes, and these were subsequently lost during the taphonomic process. The lack of the remaining bones from the right side (posterior part of the maxilla, pterygoid ectopterygoid, and posterior

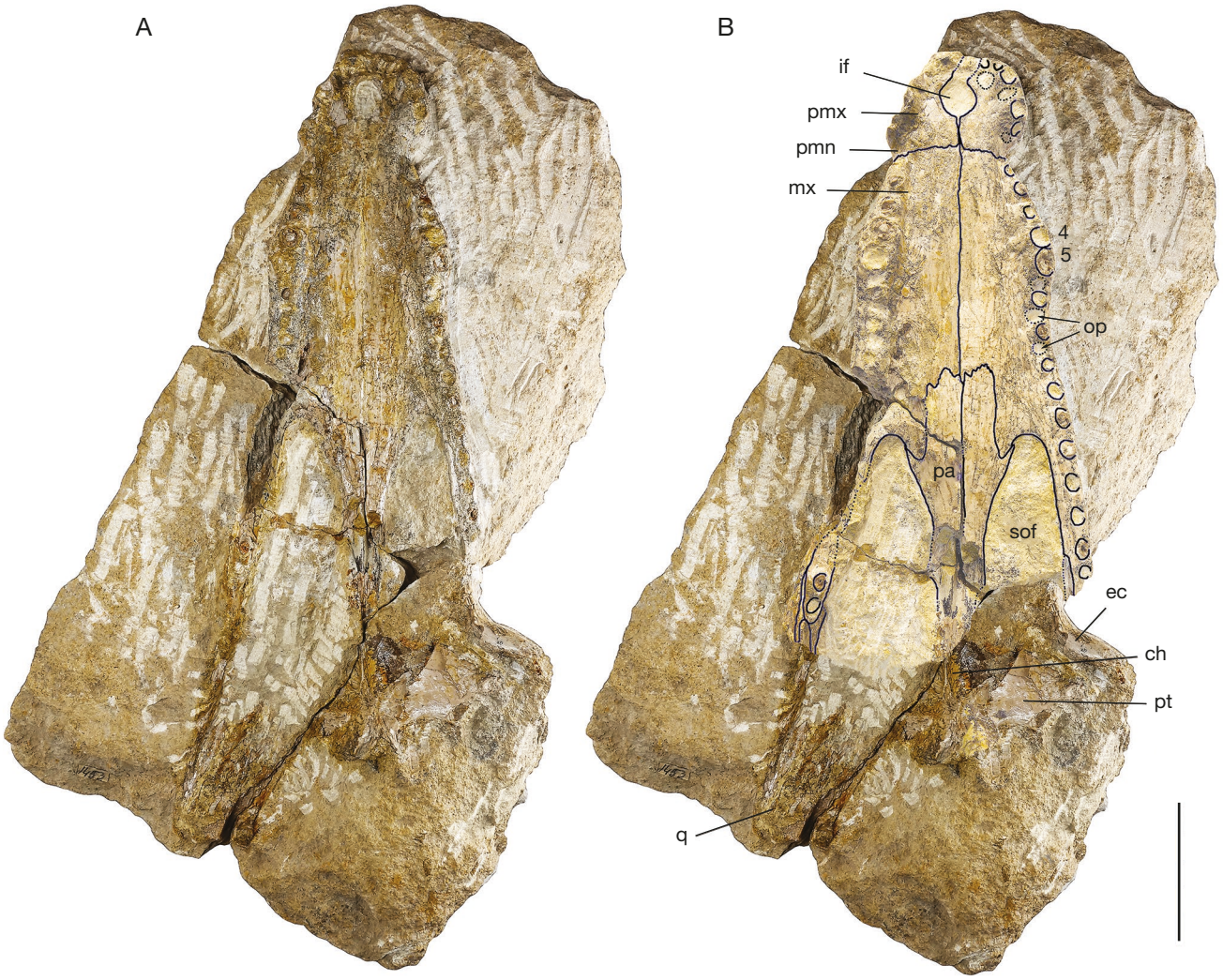

FIG. 1. — Partial skull of *Diplocynodon kochi* n. sp. from the Cluj-Mănăștur former limestone quarry, recovered in 1890: **A**, the original samples exposing the specimen in ventral view; **B**, skeletal parts highlighted. Abbreviations and numbers: **4**, **5**, fourth and fifth maxillary tooth alveoli; **ch**, choana; **ec**, ectopterygoid; **if**, incisive foramen; **mx**, maxilla; **op**, occlusal pits; **pa**, palatine; **pmn**, premaxillary-maxillary notch; **pmx**, premaxilla; **pt**, pterygoid; **q**, quadrate; **sof**, suborbital foramen. Scale bar: 5 cm.

parts of the palatines) probably is due to collecting deficiency by the quarry workers.

The photographs used in this paper were taken at the Țării Crișurilor Museum, Oradea, Romania, using a Canon EOS 5D Mark III digital camera equipped with a Canon, TS-E 24 mm lens. Parsimony analyses were conducted with the phylogenetic software package TNT version 1.1 (Goloboff *et al.* 2008). Body size estimates for the fossil specimen and related fossil alligatoroids relied on published data from Buscalioni *et al.* (1992), Delfino & Smith (2012), Godoy *et al.* (2019), Serrano-Martínez *et al.* (2019) and on the regression formulae provided by Hurlburt *et al.* (2003).

ANATOMICAL TERMS AND TAXONOMIC CONVENTIONS

Common English terms and the standard anatomical orientation system are used throughout this paper. The fossil material described herein belongs to the collections of the Geological Department Palaeontological Museum of the Babeș-Bolyai University, Cluj-Napoca, Romania.

INSTITUTIONAL ABBREVIATIONS

CAMSM	Sedgwick Museum, Cambridge;
NHMUK	Natural History Museum, London;
STUS	Sala de las Tortugas 'Emiliano Jiménez' de la Universidad de Salamanca, Salamanca;
UBB	Babeș-Bolyai University, Cluj-Napoca.

SYSTEMATIC PALAEONTOLOGY

Order CROCODYLIA Gmelin, 1789
Suborder EUSUCHIA Huxley, 1875
Superfamily ALLIGATOROIDEA Gray, 1844
Family DIPLOCYNODONTIDAE Hua, 2004

Genus *Diplocynodon* Pomel, 1847

REMARK

After Martin *et al.* (2014) the following combination of characters is diagnostic for the genus *Diplocynodon*: 1) the fourth

and fifth maxillary alveoli and the third and fourth dentary alveoli are enlarged and confluent; 2) the lacrimal is longer than the prefrontal; 3) the ectopterygoid is situated close to the posteriormost maxillary alveoli; 4) the dorsal margin of the infratemporal fenestra is bordered by the quadratojugal, preventing the quadrate from reaching the fenestra; and 5) 16-17 alveoli are present in the maxillae. Additional synapomorphy present in all members of the genus *Diplocynodon* (if preserved), identified by Rio *et al.* (2020), is that the nasals are excluded at least externally from the naris, while another two characters may be considered as ambiguous synapomorphies that are present in all *Diplocynodon* species, but also in other taxa, as follows: 1) the frontoparietal suture is linear between the supratemporal fenestrae (concavo-convex in *D. ratelii* Pomel, 1847, but linear also in *Paleosuchus*); and 2) the parietal and squamosal approach each other on the posterior wall of the supratemporal fenestrae (Rio *et al.* 2020). A single cranial autapomorphy of *Diplocynodon* has been identified by Martin *et al.* (2014): the quadrate-pterygoid suture line is linear from the basisphenoid exposure to the foramen ovale.

Diplocynodon kochi n. sp.
(Figs 1; 3-7)

urn:lsid:zoobank.org:act:C2CA2BAD-656C-4765-BB1C-50BE3CDA6A50

Derivation of name. — A tribute to Koch Antal, eminent geologist from Transylvania, Cluj-Napoca (Kolozsvár, Klausenburg), who brought an important contribution to the field of Transylvanian stratigraphy.

Holotype. — UBB V.1453, a three-dimensionally preserved, nearly complete skull lacking from its right side the anterolateral margin of premaxilla, posteriormost part of maxilla, anterior part of jugal and from its left side the postorbital, squamosal, jugal and quadratojugal.

Type locality. — Cluj-Mănăștur former limestone quarry, Cluj-Napoca, Transylvania, Romania (Fig. 2).

Stratigraphic horizon and age. — The geological strata, from where the new crocodyliform skull originates, belong to the late Eocene (Priabonian) Cluj Limestone Formation (Mészáros 2000). The stratigraphic unit consists of a series of three coarse bioclastic limestone beds rich in calcareous algae, ostracods, gastropods and bivalve shells (e.g. *Anomia tenuistriata* Deshayes, 1832) alternating with calcareous or clayey marls (Koch 1894), which were accumulated in a shallow marine carbonate platform. Occasionally, this carbonate platform emerged and was exposed to atmospheric erosion (Codrea *et al.* 1997). After Koch (1894), the main layers from the Cluj-Mănăștur limestone quarry are as follows: 1) coarse grained limestone bank (one metre thick, used as building stones or carved stones) with abundant ostracods, moulds of gastropods (mainly *Anomia tenuistriata*) and rare vertebrate remains (e.g. "*Delphinus* sp."); 2) fissured shale marlstone (0.2 meters thick) with ostracods and *Anomia*; 3) coarse grained limestone (0.5 meters thick) with ostracods and extremely small gastropods used as building stones or carved stones; 4) fissured shale marlstone (one meter thick) with ostracods and *Anomia tenuistriata*; 5) coarse grained limestone (0.8 meters thick) with ostracods and extremely small gastropods and rare *Anomia*; it represents the uppermost limestone horizon from the Cluj-Mănăștur limestone quarry; and 6) fissured shale marlstone (one meter thick) with numerous chalk-like white limestone concretions; it represents the uppermost sedimentary layer from the quarry. After Koch (1894), a partial skull of a small crocodilian consisting of "a maxilla and several inner bones of the skull" has been recovered by quarry workers. It somewhat resembled *Crocodylus communis* (i.e., *C. niloticus* Laurenti, 1768) but not identical with that because the fossil specimen possessed a higher number of teeth (21-22) vs *Crocodylus* having a lower tooth count (Koch 1894).

Diagnosis. — Small-sized late Eocene alligatoroid crocodyliform with estimated total body length up to 1.8 m. *Diplocynodon kochi* n. sp. is diagnosed within that genus by the following unique combination of characters (autapomorphy marked by *): 1) premaxillary surface with deep notch lateral to naris; 2) incisive foramen larger than half of the greatest width of premaxillae; 3) occlusion pits on the premaxillae positioned lingually to alveoli; 4) preorbital ridge prominent and wide with lateral overhang; 5) dermal bones of skull roof overhang rim of supratemporal fenestra; 6*) medial wall of parietal with deep recess; 7) anterior process of quadratojugal short; 8) margin of otic aperture inset from paroccipital process; 9) lateral carotid foramen opens dorsal to basisphenoid at maturity; and 10) posterior maxillary teeth and alveoli mediolaterally compressed.

Description of the holotype

General description

The holotype is a three-dimensionally preserved skull of a mature individual with portions of the skull damaged at the time of unearthing. The anterolateral part of the right premaxilla is broken off, whereas on the left side a small portion from the medial premaxillary border is missing; the right posterior maxillary ramus, except its posteriormost part preserving two tooth positions, is broken off; the right ectopterygoid is missing; the posterior half of the palatines and the lateral part of the right pterygoid are broken off. The damages observed on the left dorsolateral side of the skull may be related to taphonomic processes. Apparently these bones may have been lost prior to compaction of the embedding sediment as it follows: from the left postorbital only its anteromedial part in articulation with the frontal is preserved; the left squamosal is missing completely, exposing on the posterodorsal side of the otic recess and dorsal to the cranio-quadrate passage its articular surface with the underlying quadrate; the left quadratojugal and jugal are missing, from the latter only an imprint on the posterolateral side of the maxillary ramus is preserved; the left ectopterygoid is shifted anteriorly from its articulation position with the pterygoid and its anterior ramus is broken off. The outer surface of the skull is covered by a strong sculpture consisting of densely distributed, circular or irregular pits and grooves. The sculpture on the preorbital area and on the posterodorsal surface of the maxillae tends to form more elongated grooves, delimited by irregular crests. In dorsal view, the skull is elongated with a narrow snout; the preorbital length/total skull length ratio is of about 66% (Table 1). The premaxillae enclose completely the roughly circular shaped external nares that are positioned closer to the anterior premaxillary margin than to the level of the premaxillary-maxillary notch (Fig. 3). The premaxillary-maxillary notch is anteroposteriorly wide and mediolaterally shallow and flanked by prominent bony ridges that extend on the posterolateral sides of the premaxillary posterior processes. The rostrum is concave dorsally, whereas the interorbital dorsal

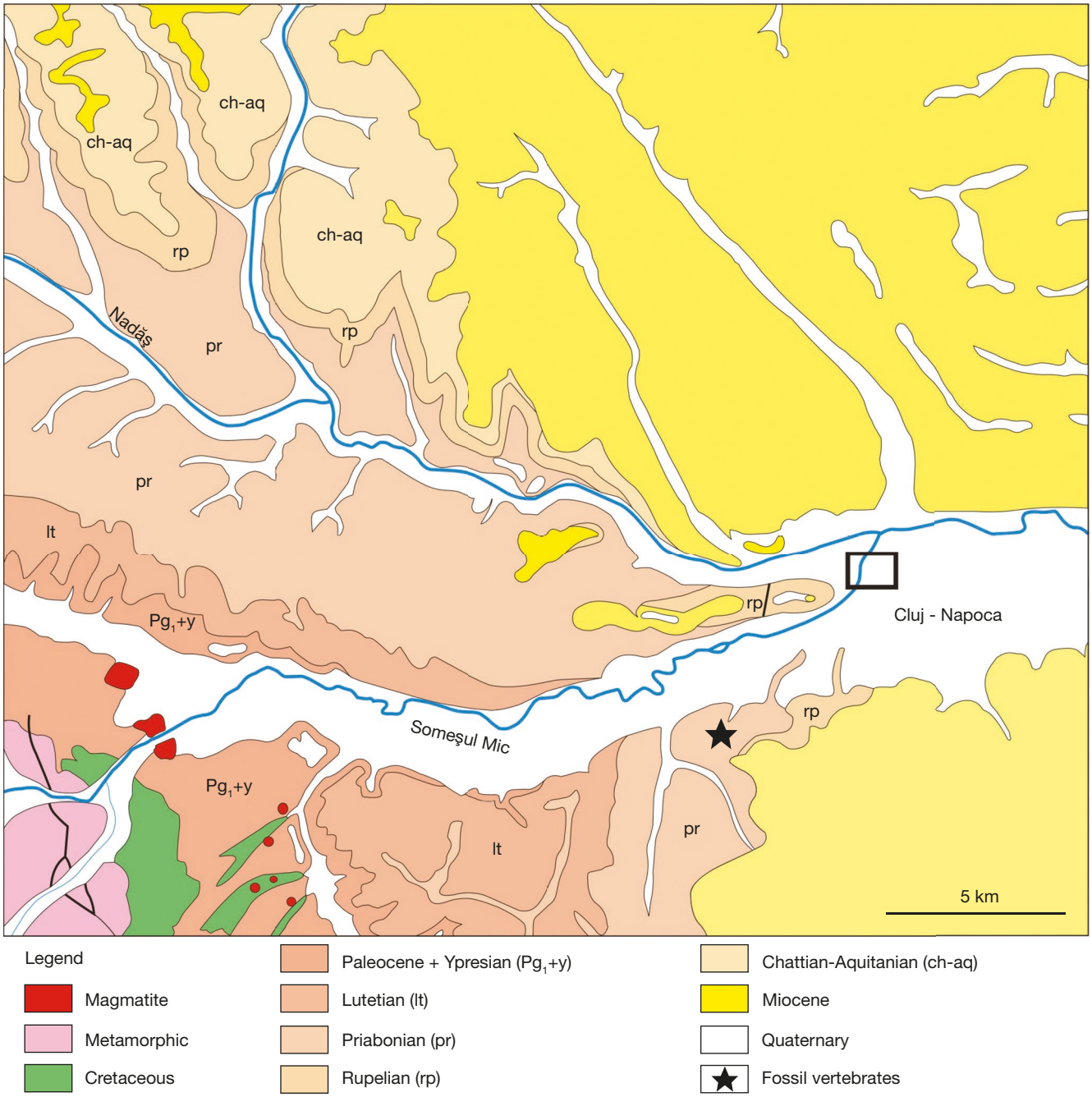

FIG. 2. — Geologic map of eastern side of Gilău sedimentary area and location of Cluj-Mănăştur fossil locality.

surface of the frontal is faintly convex. The skull table is flat and the frontoparietal suture is almost straight and situated roughly at the posterior limit of the shallower anterior portion of the supratemporal fenestra. The orbits are twice larger longitudinally than the supratemporal fenestra. The infratemporal fenestra is triangle-shaped and its posteroventral corner is bounded by the quadratojugal. In lateral view, the skull is platyrostral with the dorsal surface of the rostrum slightly curved upward, however, provided with robust and bulging premaxillary narial rims and with a dorsoventral constriction posterior to the external naris (Figs 4; 5). A wide preorbital ridge arises from the posteromedial part of the lacrimal and extends anterolaterally depicting a lateral curvature. The cranial table is formed by the postorbitals and squamosals and their fusion is situated about half-length of the supratemporal fenestra; the otic aperture is inset from the paroccipital process. The orbit is large with a strongly concave medial margin, bordered medially by the frontal and anteromedially by the prefrontal and the lacrimal. The lateral margin of the orbit is smoothly sinuous with a somewhat elevated anterolateral margin bounded by the lacrimal, whereas a less elevated posterolateral margin is bordered by the dorsally convex anterior ramus of

TABLE 1. — Skull measurements in *Diplocynodon kochi* n. sp. (mm). Symbol: *, estimation.

Skull length (premaxilla-supraoccipital)	230
Skull width (quadratojugal-quadratojugal)*	126
Preorbital length	152
Maxillary width at level of confluent teeth	57
Skull table length	45.5
Skull table width*	55
External naris length	19.2
External naris width	19
Orbital length	36
Orbital width	28
Supratemporal fenestra length	18
Supratemporal fenestra width	15
Infratemporal fenestra length	28
Infratemporal fenestra height	15.5
Suborbital fenestra length	75
Suborbital fenestra width	22
Width between orbits	10.2
Width between supratemporal fenestrae	11.2
Width between suborbital fenestrae*	13
Occipital condyle height	8
Occipital condyle width	11

the jugal representing the lower periorbital crest (Andrade & Hornung 2011); the posterior margin of the orbit is separated from the infratemporal fenestra by a pillar-like postorbital bar, resulted from the fusion of the dorsally situated flange of the postorbital with the ventrally situated and strongly inset jugal dorsal process. The infratemporal fenestra is wider and longer than the supratemporal fenestra and delimited posteriorly by the quadratojugal. In ventral view, the suborbital fenestrae are elongated and large with concave medial margins, whereas the lateral margins are almost straight (Fig. 6). Their most anterior limit reaches the level of the tenth alveolus. The suborbital fenestrae are bounded medially and anteriorly by the anteriorly widening palatines, and laterally by the maxillae, whereas posterolaterally by the anterior processes of the ectopterygoids; posteriorly these are bounded by the pterygoids. However, the articulation between the palatines and pterygoids cannot be discerned on the specimen. As a consequence, we may only presume that it was near to the posterior limit of the suborbital fenestrae, as it is seen in other members of *Diplocynodon* (Rio *et al.* 2020: fig. 2C, D). The secondary choana opens anteriorly from the posterior border of the pterygoids, however, it is strongly damaged with part of the delimiting bony laminae broken off. Fortunately, the embedding sediment preserves considerable part of the choanal morphology indicating that it has been heart-shaped with its anterior margin flush with the pterygoid surface, whereas its lateral margin is delimited by a slightly depressed area; the choanal septum is recessed within the choana (Fig. 6).

Premaxilla. The premaxillary rim, enclosing the external nares, is faintly bulging on its posterior half and bordered posterolaterally by a deep notch connected to several pits and transversal grooves; the anterior side of the premaxillary rim is flush with the narial opening. The posterior premaxillary processes extend back to the level of the third maxillary tooth positions. These processes are sutured dorsally and as a consequence the nasals are excluded broadly from the narial margins (Fig. 3).

In ventral view, the incisive foramen is relatively large (i.e., larger than half of the greatest width of the premaxillae) and oval in shape, situated at some distance from the premaxillary tooth row, where it extends between the levels of the second and fourth alveoli (Fig. 6). There are five alveoli in the premaxillae, of which the third and fourth are the largest. On the ventral side of the left premaxilla, three occlusal pits are discernible lingually to the tooth row: the first pit is larger and placed between the levels of the first and second alveoli; the second pit is smaller, placed posteromedially to the third alveolus; the third pit is small and situated posteromedially to the fifth alveolus. The suture line with the maxillae is faintly convex anteriorly, situated at the posterior border of the premaxillary-maxillary notch.

Maxilla. The outer surface of the maxillary nasal ramus is convex labially, whereas its anterolateral surface near the premaxillary fusion line is shallowly concave, as it is the posterior maxillary ramus, covered by the jugal (Fig. 3). In dorsal or ventral views, the lateral margin is produced into a lateral convexity between the first and sixth maxillary alveoli and the widest point is reached at the level of the fourth-fifth largest alveoli. The maxillary tooth row most probably included 16 teeth, of which the fourth and fifth are the largest with nearly confluent alveoli of roughly the same size; the posterior maxillary alveoli, starting from the sixth alveolus, are positioned in a straight line. As preserved, the roots or alveoli of the posteriormost teeth (positions 12th-16th) are slightly compressed mediolaterally. The occlusal pits, up to the fifth alveolus, are positioned lingually to the alveoli; the remaining occlusal pits, visible between the fifth-twelfth alveoli, are situated in line with the tooth row; posterior to the 12th maxillary alveolus, there is no trace of occlusal pit. The foramen for the palatine ramus of the fifth cranial nerve is visible on the left side, medially to the eighth maxillary alveolus (Fig. 6).

Nasal. The nasals are elongated extending from the level of the first to the 12th maxillary tooth positions (Fig. 3). The nasals are restricted anteriorly by the paired premaxillae, whereas posteriorly are sutured with the frontal medially, and with the prefrontal and lacrimal laterally.

Lacrimal. These bones are well preserved, except the anterior portion of the right lacrimal that is broken off together with the posterior ramus of the maxilla (Fig. 5A). The lacrimal is elongated and extends more anteriorly than the prefrontal, wedged between the maxilla and the nasal. The posterolateral part of the lacrimal is sutured with the jugal, whereas its posteromedial edge encloses the anterolateral margin of the orbit exposing there a smooth, boomerang-shaped surface. The preorbital ridge extends anterolaterally, arising from the smooth, posteromedial part of the lacrimal, depicting a lateral curvature, and it terminates at the level of the anterior limit of the jugal; it possesses a prominent bulging peak with a lateral overhang (Fig. 4A, C).

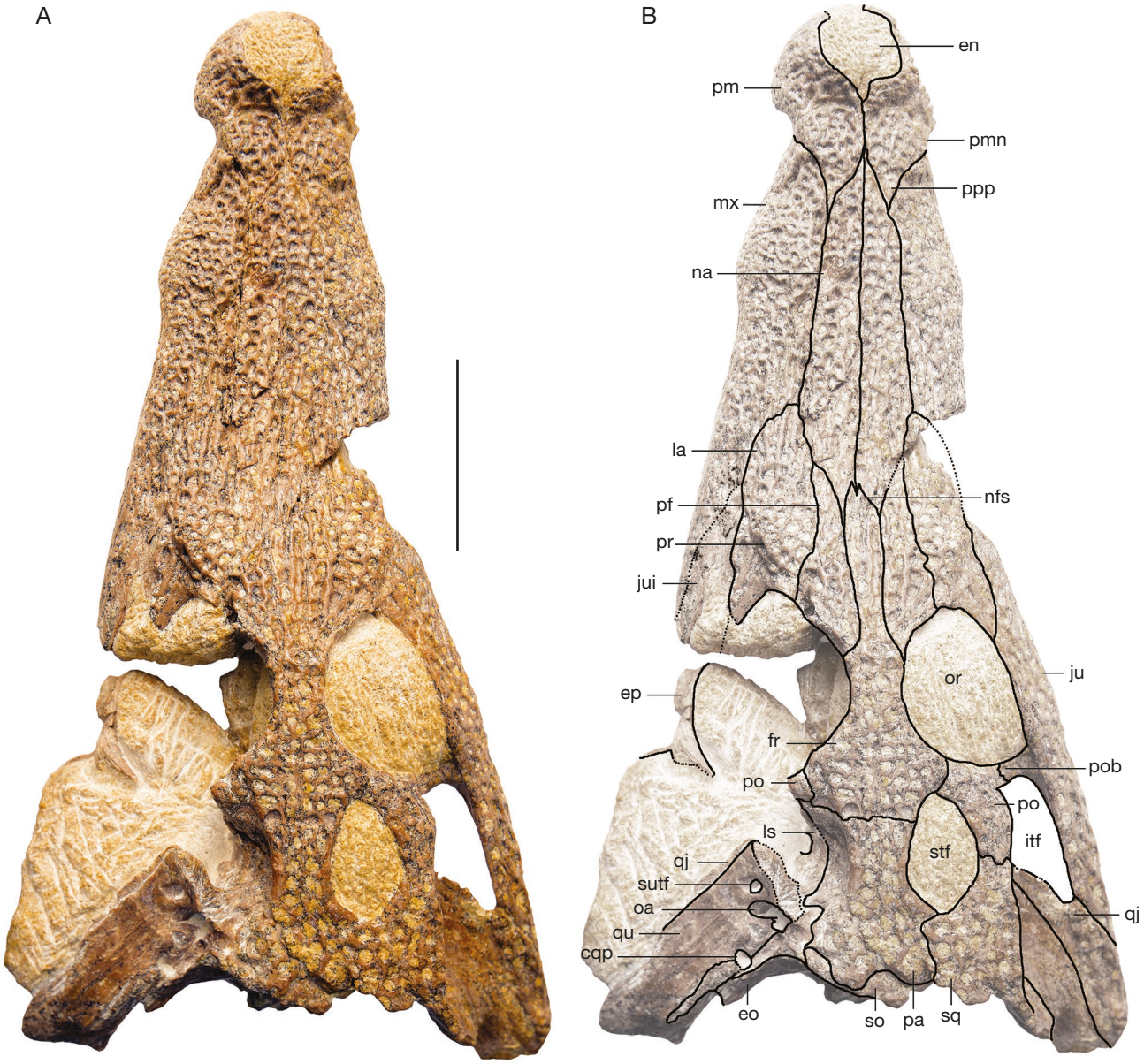

Fig. 3. — Holotype of *Diplocynodon kochi* n. sp. (UBB V.1453)*:* **A**, skull in dorsal view; **B**, skull in dorsal view with interpretive outlines. Abbreviations: **cqp**, cranio-quadrate passage; **en**, external naris; **eo**, exoccipital; **ep**, epipterygoid; **fr**, frontal; **itf**, infratemporal fenestra; **ju**, jugal; **jui**, jugal imprint; **la**, lacrimal; **ls**, latero-sfenoid; **mx**, maxilla; **na**, nasal; **nfs**, nasofrontal suture; **oa**, otic aperture; **or**, orbit; **pa**, parietal; **pf**, prefrontal; **pm**, premaxilla; **pmn**, premaxillary-maxillary notch; **po**, postorbital; **pob**, postorbital bar; **ppp**, premaxillary posterior process; **pr**, preorbital ridge; **qj**, quadratojugal; **qu**, quadrate; **so**, supraoccipital; **sq**, squamosal; **stf**, supratemporal fenestra; **sutf**, subtympanic foramen. Scale bar: 5 cm.

Prefrontal. The prefrontal is more or less a lanceolate shaped bone, tapering both anteriorly and posteriorly. Its anterior extent, positioned slightly anterior to the frontal process, is restricted by the posterior border of the nasolacrimal suture. The medial border of the prefrontal is sutured to the frontal process, whereas its posterolateral part delimits the anteromedial margin of the orbit (Fig. 3). On the left dorsolateral side, small part from the prefrontal pillar extending downward to articulate with the dorsolateral margin of the palatine is exposed.

Jugal. The jugal is an elongate and anteriorly widening bone, which delimits lateroventrally the orbit and the infratemporal fenestra. However, its greatest vertical thickness is reached at the level of its articulation point with the posterior maxillary ramus. The anterior ramus of the jugal covers dorsolaterally the maxilla with its most anterior part tapering and wedged between the maxilla and the lacrimal. Detail of this morphology is exposed on the left maxilla by an imprint of the lost anterior process of the jugal (Fig. 4A, C). The posterior ramus of the jugal, preserved on the right side only, is rod-like and articulates with the quadratojugal; the articulation point is close to the posterior corner of the infratemporal fenestra exposing a short lateral process of the quadratojugal which protrudes onto the medial surface of the jugal (Fig. 5C). On

the medial surface of the jugal, two large foramina are situated just anterior to the ascending process of the jugal and at the level of the posterior maxillary terminus respectively. The ascending process is detached medially from the body of the jugal by the dorsal crest and it is inclined dorsomedially (Fig. 3).

Frontal. The frontal is a relatively long, dagger-like bone reaching its widest point between the postorbitals (Fig. 3). There is no frontal step in the preorbital area. The rostral part is extremely thin extending anteriorly approximately to the level of the most anterior margin of the jugal. The frontal process penetrates between the posterior rami of the nasals, but it remains slightly shorter than the anterior margins of the prefrontals. Posteriorly, the articulation with the parietal is straight and the suture line extends laterally across the anterior elevated part of the supratemporal fenestra, where the parietal contacts the postorbital. The frontal bounds the anteromedial corner of the supratemporal fenestra, and its contact with the postorbital is located in the anterior margin of the supratemporal fenestra. The dorsal surface of the frontal is flat in the posterior half of the interorbital area with a slightly elevated point at the posterior orbital margin, whereas in the anterior half of the interorbital space its surface is anteroposteriorly convex and it becomes shallowly concave on the frontal process.

Postorbital. The postorbital encloses the anterolateral part of the supratemporal fenestra. It has a short and relatively thin body that is gently curved and slanting anterolaterally (Figs 3; 4A). The pillar-like postorbital bar is compressed mediolaterally and curved ventrolaterally articulating with the dorsal process of the jugal. The dorsal surface is irregular with some signs of erosion; however, the intact surface bears a strong sculpture consisting of irregular ridges and various sized pits; the sculpture extends downwards and covers also the dorsolateral part of the postorbital bar (Fig. 5A).

Parietal. The parietal bounds medially the supratemporal fenestra. Its rims are smooth, slightly raised and overhanging laterally the supratemporal fenestra, as observed on the left side of the skull (Fig. 4A, C). Below that overhang, the wall of the parietal is steeply bent medially and produced into a deep recess, probably serving as an extended insertion surface for the jaw adductor muscles (i.e., m. adductor mandibulae externus profundus – MAMEP). The parietal – squamosal contact is placed at the posterior corner of the supratemporal fenestra and their irregular suture line extends back towards the occipital margin. Near the posteromedial border, the supraoccipital prevents the parietal from reaching the occipital margin (Fig. 3). On the anterolateral margin of the supratemporal fenestra, the parietal is sutured to the medial edge of the postorbital, as seen in other members of the genus (e.g. *D. remensis* Martin *et al.,* 2014) (Martin *et al.* 2014). Anterolaterally from the posterior wall of the left supratemporal fenestra, from where the squamosal is detached from its articulating point, the dorsal surface of the quadrate is invaded by the parietal approaching close to the sutural surface left by the squamosal (Fig. 4A, C), a condition present in almost all members of *Diplocynodon* (Rio *et al.* 2020).

Squamosal. The squamosal bounds posterolaterally the supratemporal fenestra (Fig. 3). The dorsal surface is flat and wide having a relatively narrow anterior (i.e., postorbital) process. The articulation with the postorbital is about half-length of the supratemporal fenestra where the squamosal underlaps the postorbital. On the lateral margin of the squamosal, starting from the dorsally less elevated posterior prong, a roughly parallel groove for the upper ear lids extends anteriorly. The sutured line with the underlying quadrate extends from the posterolateral surface of the quadrate up to the posterodorsal side of the otic incision. In lateral view, the posterior margin of the otic aperture forms a well-defined oval recess (Fig. 5A, B), contrasting in this respect with some members of *Diplocynodon* (see Discussion), in which the posterior margin of the otic aperture is continuous with the paroccipital process (Martin *et al.* 2014).

Quadrate. The posterior quadrate rami, preserved on both sides, are elongate and moderately widened (Fig. 7A, B). The dorsal surface of the quadrate is smooth and its anterolateral margin, sutured to the quadratojugal, is flattened; anteriorly, the quadrate is restricted by the quadratojugal to enter in the infratemporal fenestra. Medially, a large concavity is divided ventrally by the otic buttress (*sensu* Montefeltro *et al.* 2016): the posterior one represents the incision of the otic aperture of the cranioquadrate passage, bounded completely by the quadrate; anterior to the cranioquadrate passage is situated the otic incision, whereas a smaller anterior opening corresponds to the subtympanic foramen (Fig. 5A). On the left side, the quadrate condyles are dorsally eroded, whereas on the right side the medial hemicondyle is broken off. The quadrate condyle consists of a ventrally deflected medial hemicondyle facing posteriorly and ventrolaterally, whereas the lateral hemicondyle has a posteroventral orientation; the foramen aëreum is situated in a shallow notch on the dorsal surface of the quadrate at some distance to the medial margin and anterior to the medial hemicondyle. In ventral view, the scar for the attachment of the adductor mandibulae posterior muscle is exposed on the posteroventral surface of the quadrate in form of a faint ridge (Fig. 6).

Quadratojugal. The quadratojugal, preserved on the right side only, is a dorsoventrally flattened bone; its dorsal surface, in line with the posterior process of the jugal, is covered by a pit and ridge sculpture resembling that of the jugal (Fig. 5A). Medially, the quadratojugal is sutured to the lateral hemicondyle of the quadrate, whereas its relatively short anterior process is sutured to the medial side of the posterior ramus of the jugal (Fig. 5C). The quadratojugal process extends along the posterior margin of the infratemporal fenestra excluding the quadrate entirely from that margin; there is no trace of a quadratojugal spine (Fig. 5C).

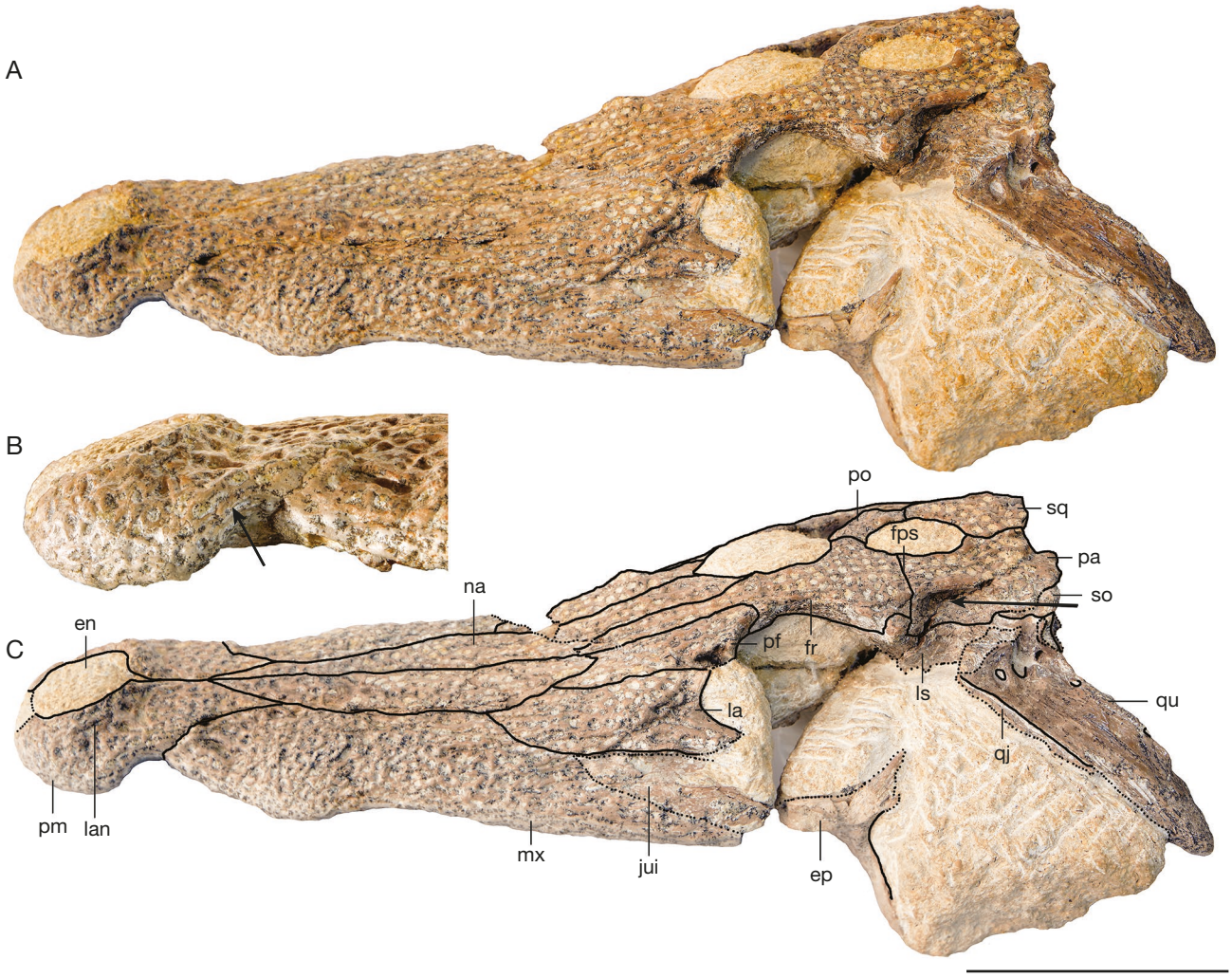

FIG. 4. — Holotype of *Diplocynodon kochi* n. sp. (UBB V.1453) in left lateral view: **A**, skull in lateral view; **B**, detail of premaxillary-maxillary constriction in lateral view. **Arrow** points to the bony ridge delimiting the premaxillary-maxillary notch; **C**, skull in lateral view with interpretive outlines. Arrow points to recess on the medial wall of the parietal. Abbreviations: **en**, external naris; **ep**, ectopterygoid; **fps**, frontoparietal suture; **fr**, frontal; **jui**, jugal imprint; **la**, lacrimal; **lan**, lateral notch on premaxilla; **ls**, laterosfenoid; **mx**, maxilla; **na**, nasal; **pa**, parietal; **pf**, prefrontal; **pm**, premaxilla; **po**, postorbital; **qj**, quadratojugal; **qu**, quadrate; **so**, supra-occipital; **sq**, squamosal. Scale bar: 5 cm.

Palatine. The anterior half of the paired palatines is preserved, whereas the posterior part is present as an imprint only (Fig. 6). The palatines form the medial margins of the suborbital fenestrae; the anterior part flares anteriorly and sends a lateral process entering into the anteromedial corner of the suborbital fenestra. The anterior flange of the palatine reaches to the level of the eighth maxillary alveolus; the suture with the maxilla is irregular and slightly convex anteriorly, the palatine underlying the maxilla at some distance. The broken surface of the palatine reveals that the choanal septum is complete, V-shaped and possesses a ventral vertical lamina that reaches the ventral surface of the palatine (Fig. 6A).

Pterygoid. The ventral part of the right pterygoid wing is completely broken off; the left wing is partially preserved (Fig. 6). The conserved parts and the imprints of the broken elements left on the embedding sediment suggest that the secondary choana was completely bounded by the pterygoid. The choanal septum is present, consisting of an extremely thin bony lamina that delimits dorsally a moderately deep embayment representing the medial and posterior corner of the secondary choana. The imprint left by the left choana is oval suggesting that the reconstructed choanae may have been heart-shaped, as in the other members of *Diplocynodon* (Rio *et al.* 2020). The posterior processes of the pterygoid are oriented posterodorsally and slightly laterally.

Ectopterygoid. The only preserved part is the anterior and posterolateral flange of the left ectopterygoid (Figs 4A, C; 6A, B). The latter is shifted anteriorly from its articulating position with the lateral wing of the pterygoid. The anterior extent of the ectopterygoid is preserved in form of an imprint on the posteromedial side of the left maxillary ramus, which demonstrates that it reached only the level of the last three

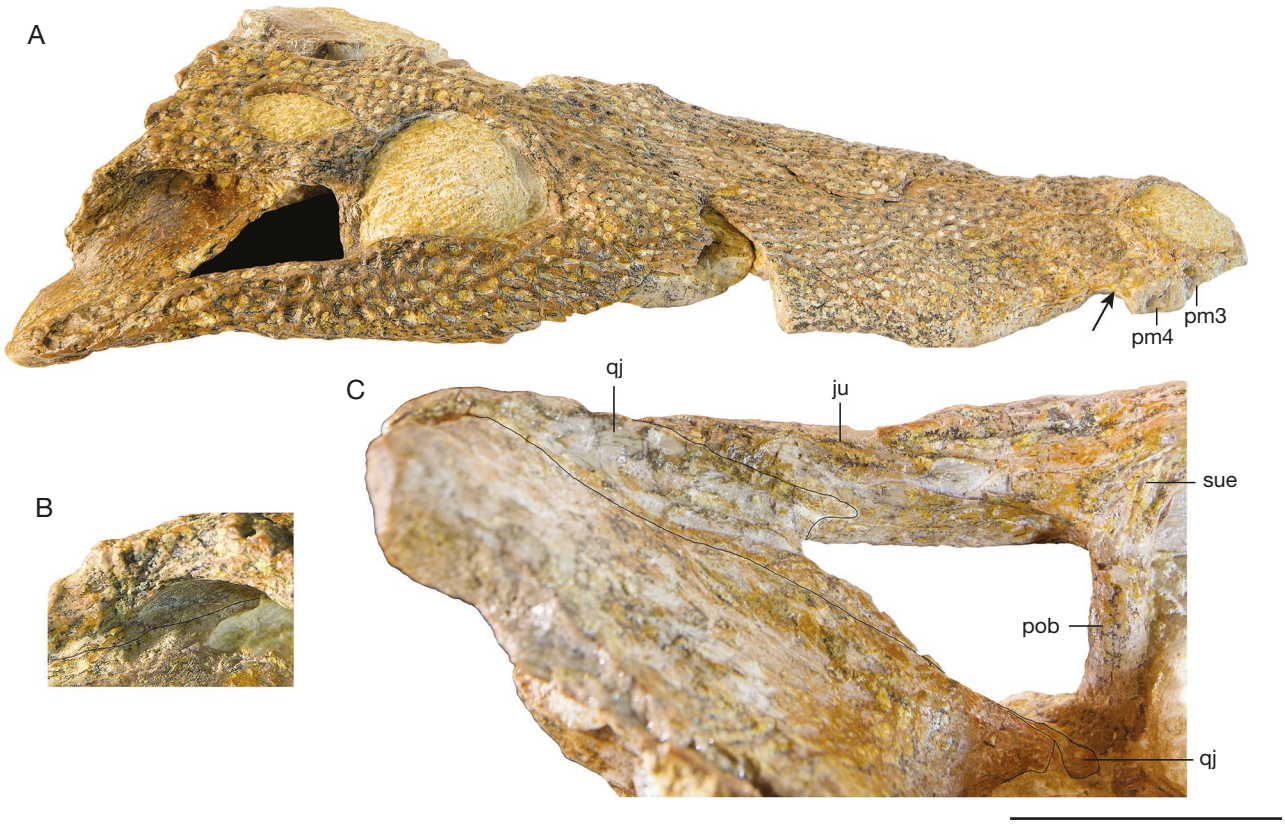

FIG. 5. — Holotype of *Diplocynodon kochi* n. sp. (UBB V.1453) in right lateral view: **A**, skull in lateral view; **B**, detail of otic aperture in lateral view; **C**, detail of infratemporal fenestra in ventral view. Abbreviations: **pm3**, **pm4**, third and fourth premaxillary tooth alveoli; **ju**, jugal; **pob**, postorbital bar; **qj**, quadratojugal; **sue**, sutural surface for ectopterygoid-jugal articulation. Arrow points to the bony ridge delimiting the premaxillary-maxillary notch. Scale bar: 5 cm.

alveoli and bordered only the last alveolus, as seen in some members of *Diplocynodon* (see below: Comparisons). The sutured surfaces, exposed on the remnant of the dorsal anterior process of the left ectopterygoid (Fig. 4A, C) and those on the medial side of the right jugal and postorbital bar (Fig. 5C), suggest that the ectopterygoid was firmly sutured to the jugal and to the base of the postorbital bar.

Supraoccipital. The supraoccipital is exposed dorsally on the medial posterior border of the occipital margin in form of a less elevated area (Fig. 3); the post-temporal fenestrae are visible on both sides of this dorsally exposed area, connected to two ventrally extending furrows; on the left side, from where the squamosal is broken off, the supraoccipital is exposed again dorsally (Fig. 7A, B). In posterior view, the supraoccipital appears as a broad triangle wedging between the sutured exoccipitals above the foramen magnum, thus being excluded from the dorsal margin of that foramen; the occipital surface is deeply concave with a low sagittal ridge on the dorsal half of the bone.

Exoccipital. The exoccipitals bound the dorsal and lateral margins of the foramen magnum (Fig. 7A, B). The lateral sides of both exoccipitals are more or less damaged. The right lateral paroccipital process is better preserved, and sutured to the prong of the squamosal dorsally and to the vertical lamina of the quadrate ventrally. The cranio-quadrate passage is exposed on the left side, enclosed dorsally by the paroccipital process; medially from that point, a prominent, but relatively short crest, that may correspond to the crista tuberalis (Serrano-Martínez *et al.* 2019), is developed at level with, but not reaching the foramen magnum. The exoccipital bears three foramina in a common recess, as follows: two small foramina, near the foramen magnum represent the exit of the paired hypoglossal nerves (cranial nerve XII); anterolaterally to these foramina, is a larger foramen representing the exit of the glossopharyngeal and vagus nerves (for cranial nerves IX-XI); ventral to this group of foramina, outside the recess enclosing the above foramina and approximately at the ventral level of the occipital condyle, is situated the lateral carotid foramen (Fig. 7C). On the dorsolateral margin of the lateral carotid foramen a sharp crest is developed and extends dorsolaterally to form the metotic crest that represents the contact area between the exoccipital and the quadrate.

Basioccipital. The basioccipital forms the floor of the foramen magnum and more ventrally it delimits the median eustachian foramen that opens between the basioccipital plate and the basisphenoid. The basioccipital condyle is of small size, whereas the basioccipital plate is slightly wider than the

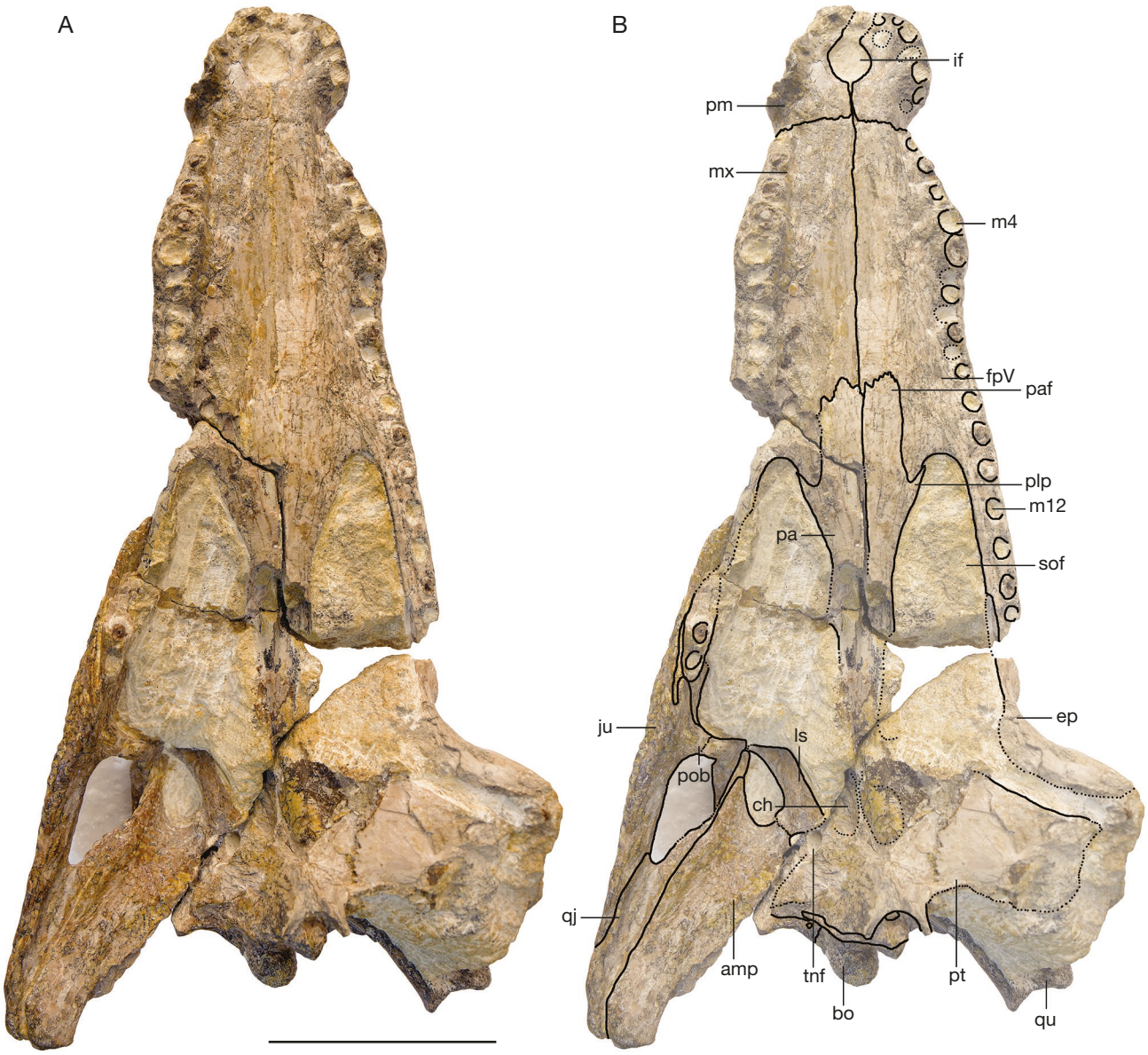

Fig. 6. — Holotype of *Diplocynodon kochi* n. sp. (UBB V.1453): **A**, skull in ventral view; **B**, skull in ventral view with interpretive outlines. Abbreviations: **amp**, scar for attachment of adductor mandibulae posterior muscle; **bo**, basioccipital; **ch**, choana; **ep**, ectopterygoid; **fpV**, foramen for the palatine ramus of fifth cranial nerve; **if**, incisive foramen; **ju**, jugal; **ls**, laterosfenoid; **m4**, fourth maxillary alveolus; **m12**, 12th maxillary alveolus; **mx**, maxilla; **pa**, palatine; **paf**, palatine anterior flange; **plp**, palatine lateral process; **pm**, premaxilla; **pob**, postorbital bar; **pt**, pterygoid; **qj**, quadratojugal; **qu**, quadrate; **sof**, suborbital fenestra; **tnf**, trigeminal nerve foramen. Scale bar: 5 cm.

condyle (Fig. 7A, B); the basioccipital plate faces posteriorly and there is a well-defined sagittal crest extending from the base of the condyle down to the ventral tuberosity; near the condyle, on both sides of the sagittal crest, the bone is pierced by tiny foramina (Fig. 7C).

Comparisons

The holotype skull of *Diplocynodon kochi* n. sp. belongs to a mature individual as indicated by the presence of strongly sutured cranial bones and the deeply ornamented dorsal surfaces of the rostrum and the skull table.

The premaxillary surface in *Diplocynodon kochi* n. sp. possesses a deep notch lateral to naris, condition present in *D. hantoniensis* Wood, 1846, *D. tormis* Buscalioni *et al.*, 1992 and *Alligator* Cuvier, 1807 (Rio *et al.* 2020), but also in *D. ratelii* (Díaz Aráez *et al.* 2017: fig. 6) and *Orientalosuchus naduongensis* Massonne *et al.*, 2019 (Massonne *et al.* 2019). In the specimen of *D.* cf. *hantoniensis*, known from the late Eocene of Mormont, W-Switzerland (Pictet 1857), regarded as Alligatoroidea indet. by Rio *et al.* (2020), the rim of the premaxilla is extremely sharp and the external naris is comparatively large, features also comparable to *D. kochi*. The posterior premaxillary process of *D. kochi* is of the same length (i.e., reaching the level of third maxillary alveolus), as that of *D. hantoniensis*, *D. muelleri* Kälin, 1936 and *D. ratelii*, whereas that of *D. remensis* reaches only the level of the

second maxillary alveolus (Martin *et al.* 2014). In contrast, in some Asian alligatoroids (e.g. *Orientalosuchus naduongensis* Massonne *et al.*, 2019) the posterior premaxillary process extends posterior to the level of the fourth maxillary alveolus (Massone *et al.* 2019), whereas in some North American taxa (e.g. *Brachychampsa*), it may extend into the level of the fifth maxillary alveolus (Mook 1925). In the premaxilla of *D. kochi* the third and fourth alveoli are the largest, similar to *D. hantoniensis* and *D. remensis* (Martin *et al.* 2014). Three occlusal pits are observed in the premaxillae of *D. kochi* positioned lingually to the alveoli, condition somewhat similar to *D. hantoniensis* (Rio *et al.* 2020), *D. remensis* (Martin *et al.* 2014) and *D. muelleri* (Piras & Buscalioni 2006), whereas in *D. tormis* and *D. ratelii* the occlusal pits are interlocked between the premaxillary teeth (Piras & Buscalioni 2006). The incisive foramen in *D. kochi* is larger than half of the greatest width of the premaxillae, whereas it is small in the remaining members of *Diplocynodon*. The nasals in *D. kochi*, similarly to most members of the genus *Diplocynodon*, are excluded from the naris, as it is seen also in *Borealosuchus* (Brochu 1999, 2000; Wu *et al.* 2001). In *D. ratelii* the nasals reach the external naris (Díaz Aráez *et al.* 2017; Luján *et al.* 2019), whereas in *D. darwini* the nasals almost contact the naris (Brochu 1999: fig. 32; Martin *et al.* 2014).

In *D. kochi*, the anteroposteriorly wide and mediolaterally shallow premaxillary-maxillary notch is bordered laterally by a bony ridge extending on the dorsolateral surface of the posterior premaxillary process. The resulting anterior margin of this notch stands roughly in an angle of 30° with the sagittal plane as opposed to the condition seen in some members of *Diplocynodon* (e.g. *D. remensis*) where the lateral margins of the premaxillae become perpendicular to the sagittal plane (Martin *et al.* 2014). The premaxillary-maxillary notch in *D. muelleri*, *D. deponiae* Frey *et al.*, 1987 and *D. hantoniensis* is rather small or absent (Piras & Buscalioni 2006; Delfino & Smith 2012; Macaluso *et al.* 2019; Rio *et al.* 2020). In the remaining members of the genus, including *D. darwini, D. ratelii, D. tormis*, *D. ungeri* Prangner, 1845 and *D. remensis* the above constriction is present, but its morphology may be subject to ontogenetic variation. The bony ridge bordering the premaxillary-maxillary notch in *D. kochi* is positioned on the dorsolateral side of the premaxillary-maxillary notch, whereas in *D. remensis* two parallel ridges are positioned deeply within that notch, just posterior to the fifth premaxillary alveolus (Martin *et al.* 2014), and that part seemingly is remodelled ontogenetically by the enlarged dentary teeth.

The occlusion pits in the maxilla are distributed variably in the members of the genus, *D. kochi* resembling *D. ratelii*, *D. tormis* and *D. muelleri*, where the dentary teeth occlude in line with the maxillary toothrow (Díaz Aráez *et al.* 2017; Massone *et al.* 2019). The maxillary teeth and alveoli in *D. kochi*, up to the 11th tooth position, are more or less circular in shape, whereas the last five teeth and/or alveoli are slightly compressed mediolaterally, condition present also in *D. remensis* (Martin *et al.* 2014) and *Brachychampsa montana* Gilmore, 1911 (Mook 1925).

The anterior extent of the anterior process of the frontal in *D. darwini* is shorter than that of the jugal (Hastings & Hellmund 2015: fig. 2), whereas it is approximately the same in *D. hantoniensis*, (e.g. in NHMUK OR 25170) (Rio *et al.* 2020), *D. kochi* (Fig. 3B) and *D. tormis* (Massone *et al.* 2019). Nevertheless, the anterior extent of the jugal is shorter than that of the frontal in *D. remensis* (Martin *et al.* 2014: fig. 2), *D. ratelii* (Díaz Aráez *et al.* 2017: fig. 3) and *D. muelleri* (Massone *et al.* 2019). The frontal of *D. kochi* lacks a preorbital step; it is also absent or weakly developed in *D. hantoniensis*, *D. darwini*, *D. deponiae* and *D. ratelii* (Rio *et al.* 2020), but it has been described in *D. remensis* (Martin *et al.* 2014), and figured in *D. tormis* (Buscalioni *et al.* 1992: fig. 2); the specimen STUS-344 of *D. tormis* apparently lacks any trace of this step in the preorbital area (Serrano-Martínez *et al.* 2019: fig. 1E).

The dorsal sculpture of *D. kochi* in the preorbital area approaches the condition seen in *D. tormis*, the latter possessing three short grooves: one is sagittal extending on the frontal process, while the other two extend anterolaterally, parallel with the orbital margins (Serrano-Martínez *et al.* 2019). However, the frontal process in the holotype of *D.* tormis, as reported by Buscalioni *et al.* (1992), is devoid of dorsal sculpture, probably representing an intraspecific variation. The preorbital ridge in *D. kochi* is wide but prominent and possesses a lateral overhang, however it is relatively short and restricted only to the surface of the lacrimal. In *D. remensis* a preorbital ridge has been reported by Martin *et al.* (2014: 877), but considered as weakly developed and therefore displaying the plesiomorphic condition. In *Orientalosuchus naduongensis*, the preorbital ridge is prominent, as it is in *Krabisuchus* Martin & Lauprasert, 2010, *Mourasuchus* Price, 1964 and some crocodylids, and connected anteriorly to a prominent ridge developed on the maxilla (Massone *et al.* 2019).

The dorsolateral part of the postorbital bar is sculptured in *D. kochi* and *D. hantoniensis*, whereas in *D. tormis* that surface is entirely smooth and delimited dorsally by a sharp ridge (Buscalioni *et al.* 1992; Serrano-Martínez *et al.* 2019: fig. 1E).

The supratemporal margin of the parietal in *D. kochi* is produced into a wide overhang and the medial wall of the parietal is deeply inset forming a deep recess, probably serving as an extended shelf-like insertion surface for the specific jaw adductor muscles (MAMEP) being in control for rapid closure of the lower jaws in a palinal type jaw movement (Holliday & Witmer 2007; Ősi 2014).

The morphology of the most posterior margin of the right maxilla and the imprint left by the left ectopterygoid on the medial side of left posterior maxillary ramus suggest that the ectopterygoid may have bordered only the last maxillary alveolus, whereas the next two alveoli were delimited by the maxilla, condition very similar to *D. ratelii* (Rio *et al.* 2020: fig. 29D).

The anterior process of the quadratojugal is short, extending as a triangular process onto the medial surface of the jugal, a character contrasting with the remaining members of *Diplocynodon*, where it is known (e.g. *D. darwini*, *D. deponiae*, *D. ratelii*, *D. tormis*). In *D. kochi*, the quadratojugal spine

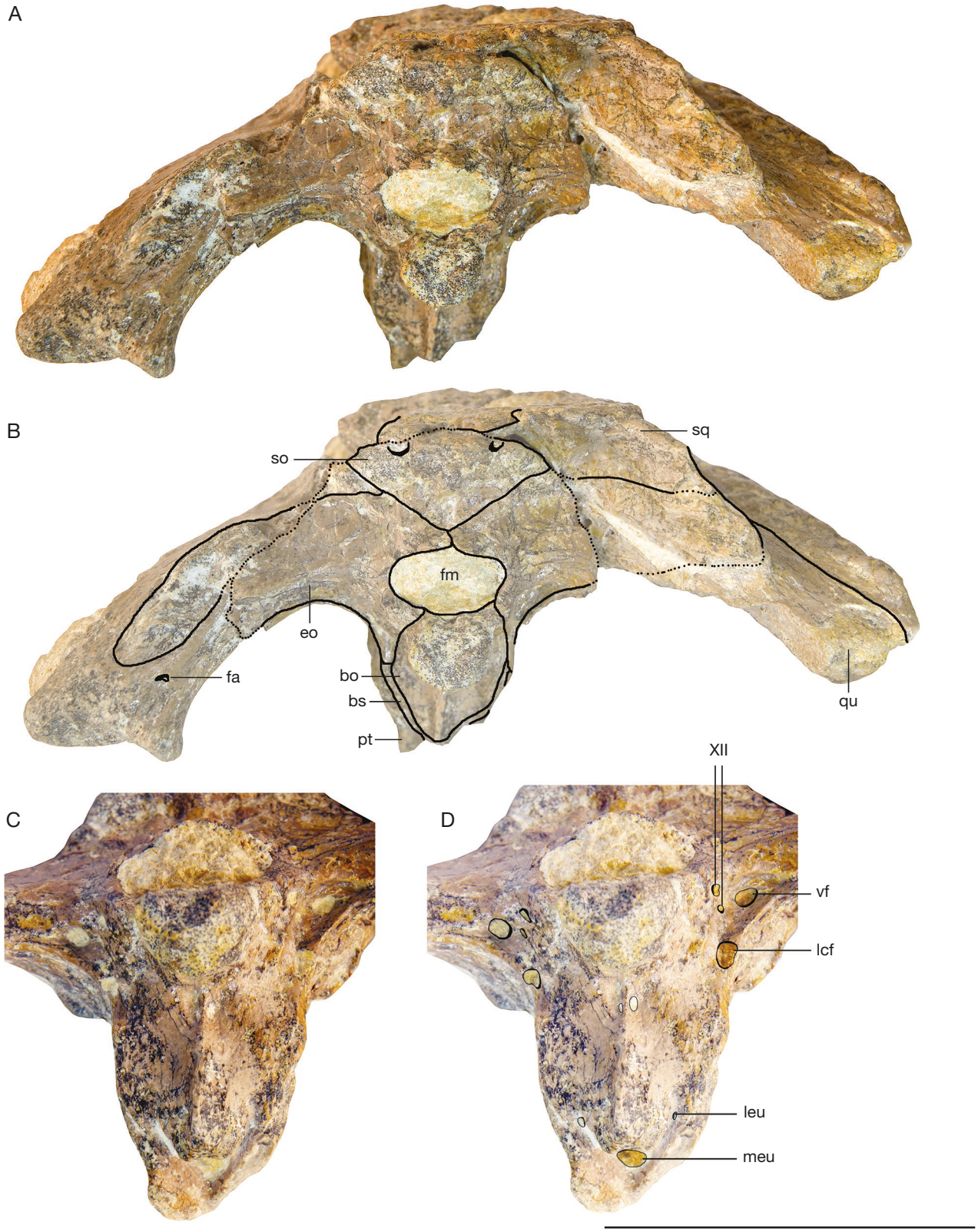

FIG. 7. — Holotype of *Diplocynodon kochi* n. sp. (UBB V.1453): **A**, skull in posterior view; **B**, skull in posterior view with interpretive outlines; **C**, detail of basioccipital area in posteroventral view; **D**, detail of basioccipital area in posteroventral view with interpretive outlines. Abbreviations: **bo**, basioccipital; **bs**, basisphenoid; **eo**, exoccipital; **fa**, foramen aëreum; **fm**, foramen magnum; **lcf**, lateral carotid foramen; **leu**, lateral eustachian opening; **meu**, medial eustachian opening; **pt**, pterygoid; **qu**, quadrate; **so**, supraoccipital; **sq**, squamosal, **vf**, vagus foramen; **XII**, hypoglossal nerve foramen. Scale bar: 5 cm.

is not preserved, but the available part of the quadratojugal process extending along the posterior margin of the infratemporal fenestra remains more or less parallel suggesting that it has been devoid of this structure, as in other members of the genus.

The posterior margin of the otic aperture in *D. kochi* is inset similarly to *D. darwini* (Massone *et al.* 2019), *D. hantoniensis* (Rio *et al.* 2020: fig. 3A, B) and *D. tormis* (Serrano-Martínez *et al.* 2019: fig. 1A). This condition contrasts with that of the remaining members of the genus (if preserved), where the posterior margin of the otic aperture is flush with the paroccipital process, as it is observed in *D. remensis* (Martin *et al.* 2014: fig. 3A, B, D) and *D. deponiae* (Delfino & Smith 2012: fig. 4).

The position of the lateral carotid foramen, situated above the dorsal margin of the basisphenoid, is similar to the condition known in *D. tormis* (Serrano-Martínez *et al.* 2019: figs 1D; 2F), but also to *Asiatosuchus depressifrons* Blainville, 1855 (Delfino & Smith 2009) and crocodylids (see below). However, in the remaining members of the genus *Diplocynodon* (if known), the lateral carotid foramen opens laterally to the basisphenoid (Martin *et al.* 2014; Massone *et al.* 2019; Rio *et al.* 2020: fig. 3D), this trait representing the plesiomorphic condition.

Phylogenetic analysis

Character-taxon matrix and analytical protocol

We added all the scored osteological characters of *Diplocynodon kochi* n. sp. (106 characters, representing 53% from the character list) to the character-taxon matrix (CTM) of Massone *et al.* (2019) consisting of 115 operational taxonomic units (OTU) and 202 phenotypic characters. The dataset of these authors, based on the original dataset of Brochu & Storrs (2012), was amended and new characters were added from Wang *et al.* (2016), Cossette & Brochu (2018) and Li *et al.* (2019), using *Bernissartia fagesii* Dollo, 1883 as the outgroup. The original CTM of Massone *et al.* (2019) was reduced by us to 77 OTUs (including *D. kochi* n. sp. and *D. remensis*) and to 199 phenotypic characters (i.e., without the last three characters, considered irrelevant for the present study). We also applied the emendations proposed to the original dataset by Massone *et al.* (2019: supplementary material); all the characters were treated as unordered. We performed a parsimony analysis using the TNT version 1.1 of Goloboff *et al.* (2008), in which the CTM was first analysed using the 'New Tehnology search' option with the sectorial search, ratchet, tree drift and tree fusing options as default parameters. A search for suboptimal trees ten steps longer than that of the most parsimonious tree was also completed to calculate the decay indices of Bremer (1994) and the common synapomorphies for all trees were also mapped in the 'Optimize' menu.

RESULTS

In the analysis, the TNT returned six parsimonious trees of 812 steps from a total of 23.733.392 rearrangement examined (consistency index [CI] = 0.322; retention index [RI] = 0.739; homoplasy index [HI] = 0.678; rescaled consistency index [RCI] = 0.237). The strict consensus tree depicts Diplocynodontidae as a monophyletic clade, where *Diplocynodon deponiae* and *D. darwini* are recovered in a successively nesting position, while *D. kochi* n. sp. appears as a terminal taxon and the sister-species to the coeval *D. tormis* (Fig. 8); the topology within this clade remains unchanged in all six trees. The basal split within Alligatoroidea occurs between Diplocynodontidae and the remaining alligatoroids, where the diplocynodontids appears as the sister taxon to Globidonta. Nodal support is moderate for Brevirostres (decay index = 3) and Alligatoroidea (decay index = 3), and relatively weak for Diplocynodontidae (decay index = 2).

Leidyosuchus canadiensis Lambe, 1907, considered the most basal alligatoroid (e.g. Brochu 1999, 2004; Wang *et al.* 2016; Suess 2019), is positioned crown-ward and recovered with *Deinosuchus* in an unresolved relationship within Globidonta Brochu, 1999. According to Massone *et al.* (2019) the shift of *Leidyosuchus* into a more crown-ward position is resulted from one of their newly applied characters (Massone *et al.* 2019: supplementary file, character 195). However, in our analysis Globidonta is supported only by a single common synapomorphy: the frontoparietal suture is concavo-convex (ch. 151-0), while on some trees by another character, the lingual foramen for articular artery and alveolar nerve perforates surangular entirely (ch. 69-0); the third character (ch. 195-0), reported by Massone *et al.* (2019), unfortunately was not mapped in our analysis. The list of common synapomorphies (supporting the clade of Alligatoroidea) is the same as in the analysis of Massone *et al.* (2019: supplementary file), except the character 104 (1), which was not mapped in our analysis. Of this list of characters, only two synapomorphies were recorded in *D. kochi* n. sp. supporting its inclusion within that clade: anterior tip of frontal forms broad, complex sutural contact with the nasals (ch. 131-1) and quadrate foramen aëreum is located on the dorsal surface of quadrate (ch. 177-1). The clade of Diplocynodontidae is supported by three synapomorphies: axial hypapophysis located toward the center of centrum (ch. 15-0), presence of paired ventral ossifications that suture together (ch. 42-2) and quadratojugal spine is greatly reduced or absent at maturity (ch. 140-1). Finally, within Diplocynodontidae, the clade of (*D. kochi* + *D. tormis*) is supported by a single synapomorphy: lateral carotid foramen opens dorsal to basisphenoid at maturity (ch. 169-1).

The most important results of the parsimony analysis are that in all the most parsimonious trees, Diplocynodontidae are recovered as a monophyletic clade, and that among intrageneric members the relationships appear fully resolved. *Diplocynodon kochi* n. sp., despite its older geologic age (versus *D. muelleri*, known from the Oligocene; *D. ratelii*, known from the Oligocene and Miocene; *D. ungeri*, known from the Miocene) (see Rio *et al.* 2020 and references therein), represents one of the most derived members of that genus. Several derived or autapomorphic traits in *D. kochi* n. sp., seen on its premaxilla [nasals are excluded from the naris (ch. 82-1),

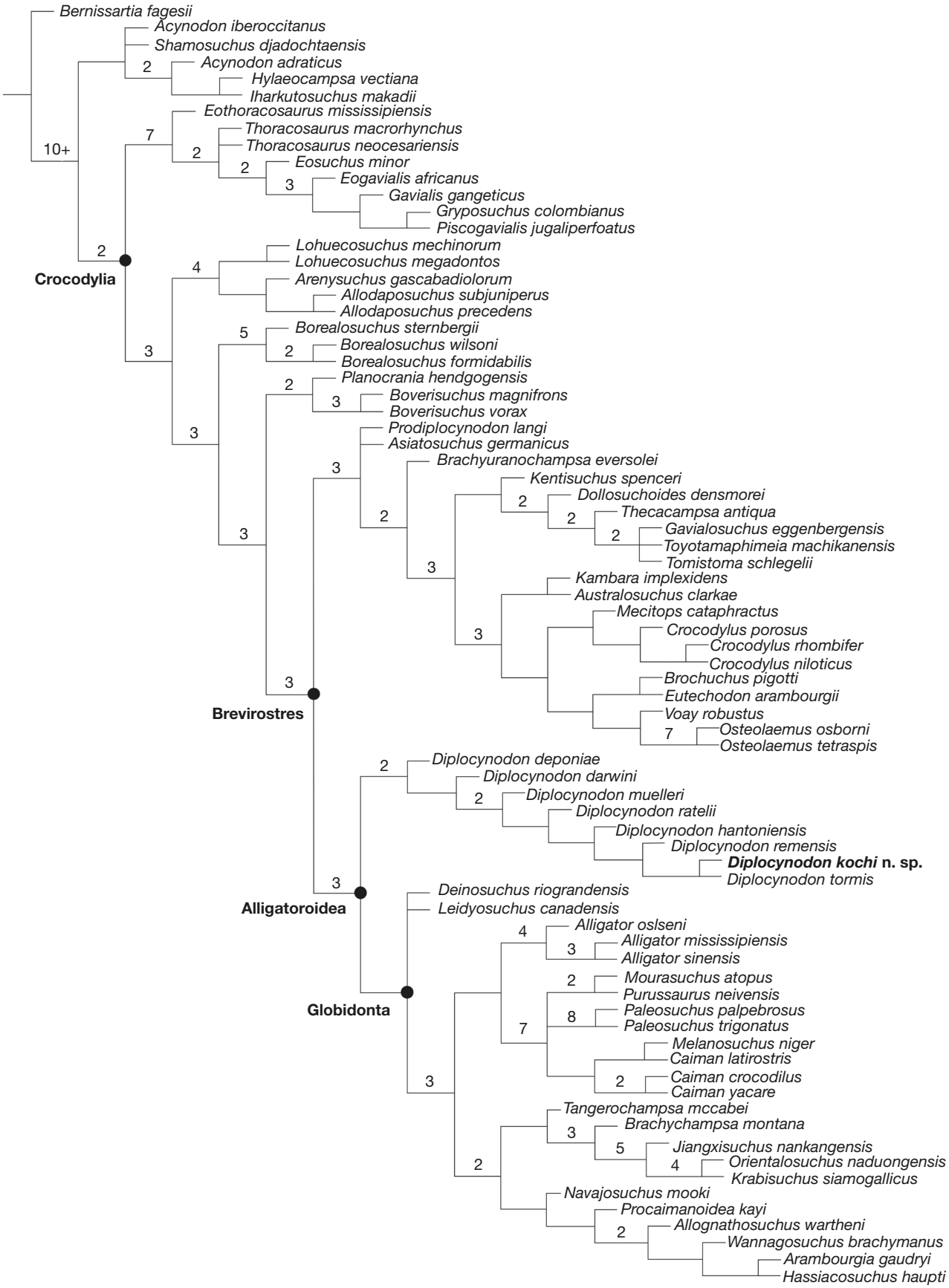

Fig. 8. — Relationships of *Diplocynodon kochi* n. sp., based on our phylogenetic analysis. Strict consensus tree resulting from six most parsimonious trees generated by TNT, based on 77 OTUs with 199 phenotypic characters [derived from Massone *et al.* 2019]. Numbers above nodes indicate decay indices of Bremer (= extra steps).

incisive foramen is large, more than half the greatest width of premaxillae (ch. 88-1), third and fourth premaxillary alveoli are the largest (ch. 190-3)], maxilla [posterior teeth and alveoli laterally compressed (ch. 79-1)] and parietal [skull roof overhang rim of supratemporal fenestra (ch. 152-1), parietal medial wall forms a deep recess] may have been related to its peculiar life style (see below).

DISCUSSION

Taxonomic identification of *Diplocynodon kochi* n. sp.

Based on our parsimony analysis *D. kochi* n. sp. is recovered as the sister taxon of *D. tormis*, the latter known from the middle Eocene Areniscas de Cabrerizos Formation, Salamanca, Spain. The skull range of *D. kochi* n. sp and *D. tormis* correspond to a medium body size category (see below) and their snout profile is rather similar, of relatively narrow, platyrostral type and provided with a shallow premaxillary-maxillary constriction (ch. 196-0). In both the above taxa (also in *D. hantoniensis* and *D. ratelii*), the naris is delimited posterolaterally by a deep notch (ch. 86-1) (Rio *et al.* 2020), whereas the lateral carotid foramen opens dorsal to basisphenoid at maturity (ch. 169-1). In contrast, phenotypic disparity between *D. kochi* n. sp and its congeners is more conspicuous, documenting its less inclusive position within the clade of Diplocynodontidae. The occlusal pits in the premaxillae of *D. tormis* and *D. ratelii* are interlocked between the alveoli (Piras & Buscalioni 2006) contrasting with the remaining members (including *D. kochi* n. sp), where these are positioned lingually to the alveoli. The preorbital ridge in *D. kochi* n. sp is prominent, wide and developed into a lateral overhang, whereas in *D. remensis* it is present, but weakly defined; the preorbital ridge is lacking in the remaining congeners. In both *D. kochi* n. sp and *D. deponiae,* the skull roof overhangs the rim of the supratemporal fenestra near maturity (ch. 152-1), whereas in the other congeners, the skull roof does not overhang rim at maturity (ch. 152-0). The medial wall of the parietal in *D. kochi* n. sp is produced into a deep recess (autapomorphic trait), probably serving as an extended insertion surface for the jaw adductor muscles.

Life style of *Diplocynodon kochi* n. sp.

The skull of *D. kochi* n. sp represents the first example of a diplocynodontid discovered in a marine taphonomic context. The specimen, beyond collecting deficiencies (the sample was broken in three parts and subsequently portions of the skull has been lost), is well-preserved, devoid of any signs of destruction on the outer surface, suggesting that prior to its burial, it experienced a short transport and was subsequently deposited in a shallow marine sedimentary environment. Fortunately, the skull has retained its original tridimensional shape after being embedded into loose skeletal sediment, mainly consisting of ostracod and mollusc shells and transformed in time into bioclastic limestone.

Reconstructed body size estimation, based on Hurlburt *et al.* (2003) and Godoy *et al.* (2019: additional files 1, 2), indicates that *D. kochi* n. sp was a medium-sized alligatoroid (dorsal cranial length (DCL) = 0.23 m, total length (TL) = 1.76 m, being in range of *D. tormis* (1.4-1.8 m) and *D. darwini* (1.4-1.8 m). Among the remaining members of the genus, *D. hantoniensis* was probably the largest (DCL of the skull CAMSM TN 917 = 0.376, TL = 2.9 m), whereas the available specimens of *D. deponiae* were the smallest (DCL = 0.95-0.108 m; TL = 0.73-0.83 m) (see also Delfino & Smith 2012).

Despite its occurrence in marine sedimentary environment, the osmoregulation of *D. kochi* n. sp in saline water probably was rather limited and comparable to recent alligatorids, the latter group lacking lingual salt glands responsible for salt and water balance in seawater (Grigg & Kirschner 2015: 416). In contrary, recent crocodylids (e.g. *Crocodylus porosus* Schneider, 1801), possessing lingual salt glands (Taplin 1988), are able to maintain their salt and water balance in fully marine conditions, and as a consequence, they can live longer period in seawater, tolerating even hypersaline situations (Taplin 1984). It is assumed that salt water tolerance is plesiomorphic in Eusuchia, thus the ancestors of recent alligatorids could have lost their marine capability during the Mesozoic (Wheatley 2010; Wheatley *et al.* 2012). According to Brochu (2001), it is not known if *Diplocynodon* was salt-tolerant or not, since it is not a member of the crown-group Alligatoridae. However, an indirect evidence for a limited salt water tolerance of diplocynodontids and of other alligatoroids may rely on their low capacity of documented transoceanic colonisation (Delfino *et al.* 2007). Nevertheless, large sized individuals of *Alligator mississippiensis* Daudin, 1802 have been observed in brackish situations bordering freshwater marshes or occasionally in the sea at considerable distance (more than 60 km) from the coastline (Grigg & Kirschner 2015). Such a scenario could have been possible for large mature individuals of *D. kochi* n. sp surveying the sea-water near the shoreline. The slender, platyrostral snout, the extended insertion surface for external jaw adductors (MAMEP) in the supratemporal fossa (i.e., enlarged medio-posterior shelf on the parietal and squamosal) (Fig. 4A, C), and the mediolaterally slightly compressed posterior teeth are good indicators for an active hunt of *D. kochi* n. sp. The rapid jaw movement during the bite is ensured by the external adductors pulling the mandibles simultaneously upwards and backward and bringing the upper and lower teeth into a shearing contact (Ősi 2014). Potential prey for *D. kochi* n. sp of adequate size could include both invertebrates and smaller vertebrates occurring in shallow waters. Beside this unique alligatoroid specimen, other vertebrates recorded from Cluj-Mănăștur locality include turtles, like *'Trionyx' clavatomarginatus* Lörenthey, 1903 (Farkas 1995), sulid birds, like *Eostega lebedinskyi* Lambrecht, 1929 (Mlíkovský 2007) and the more frequent sirenians (Fărcaș & Codrea 2008; Fărcaș 2011), representing probably *Protosiren* (Diedrich 2013).

In conclusion, *D. kochi* n. sp most probably entered only occasionally into the seawater, the species main preference remaining freshwater habitats, as such a taphonomic context (i.e., fluviatile) is known from the late Eocene (Priabonian) of Rădaia, that locality yielding isolated remains of crocodilians (Codrea & Venczel 2020).

Palaeobiogeographic implications

Diplocynodon kochi n. sp is the first late Eocene crocodilian taxon ever described from Romania in the last 130 years and the only skull of that group discovered from the Gilău sedimentary area. Moreover, so far, it is the easternmost European occurrence of a diplocynodontid and the first example of its clade reported from fully marine sedimentary rocks.

Most fossil records of the European endemic *Diplocynodon* are known from the western part of the continent, of which five members are identified from the Eocene: *D. tormis* is known from the early Eocene to the early Oligocene of Spain (Buscalioni *et al.* 1992); *D. darwini* and *D. deponiae*, are known from the middle Eocene of Germany (Rossmann & Blume 1999; Delfino & Smith 2012); *D. hantoniensis* and *D. elavericus* Martin, 2010 are known from the late Eocene of England and France (Martin 2010; Rio *et al.* 2020). In regards to the late Eocene (Priabonian) *D. kochi* n. sp., we may presume also a western European origin, considering its phenotypic resemblance with *D. tormis*.

The colonisation of the eastern part of the continent or a faunal interchange for some tetrapod taxa may have been a slow process, if we take into account that during the Eocene the eustatic level was extremely high and Europe still looked as an archipelago with extensive epicontinental seas and temporarily interconnected landmasses (Rage & Roček 2003). The fossil record of *D. kochi* n. sp from Cluj-Mănăștur locality indicates that during the late Eocene (Priabonian) *Diplocynodon* colonised already the eastern side of Central Europe and probably it was able to survive amid deteriorating climatic conditions the Eocene/Oligocene boundary, since it was recorded also from the early Oligocene (Rupelian) localities of Suceag and Cetățuia Hill, Cluj-Napoca (Fărcaș 2011; Codrea & Venczel 2020). Southward migration of *Diplocynodon* during the Eocene – Oligocene transition (EOT), as proposed by Martin (2010), appears less probable, since no large climatic pressure persisted during the EOT, that enabled the survival of *Diplocynodon* populations in their original habitats even in more northern European localities (e.g. in NW Bohemia) (Chroust *et al.* 2019).

CONCLUSIONS

1) *Diplocynodon kochi* n. sp., is the first late Eocene crocodilian taxon ever described from Romania and the only alligatoroid found in marine taphonomic context.

2) Our parsimony analysis confirms the monophyletic status of diplocynodontids; on all most parsimonious trees, *D. kochi* n. sp., appears as the sister taxon of *D. tormis*.

3) Comparable to recent alligatorids, *D. kochi* n. sp., preferred probably freshwater habitats and it might have occurred only occasionally in seawater.

4) The fossil record of *D. kochi* n. sp., from the late Eocene (Priabonian) of eastern side of Central Europe suggests that *Diplocynodon* colonised a considerable part of the European territory from West to East; the early Oligocene (Rupelian) fossil records from the area suggest that the genus survived the Eocene – Oligocene transition in its original habitats, despite of deteriorating climatic condition at the Eocene/Oligocene boundary.

Acknowledgements

The geological map of the eastern part of Gilău sedimentary area was produced by Dr Cristina Fărcaș. Curator Dr Liana Săsăran from the Paleontological Museum of UBB, Cluj-Napoca, kindly allowed us the examination of *Diplocynodon kochi* n. sp specimen hosted in their museum. We thank Dr. Thierry Smith for his help in correcting the French abstract. We also thank Dr Massimo Delfino and the anonymous reviewer for their critical comments and suggestions that greatly improved the paper. Thanks are also due to Dr Éric Buffetaut and Fariza Sissi for additional guidance and editorial assistance.

REFERENCES

Andrade M. B. & Hornung J. J. 2011. — A new look into the periorbital morphology of *Goniopholis* (Mesoeucrocodylia: Neosuchia) and related forms. *Journal of Vertebrate Paleontology* 31: 352-368. https://doi.org/10.1080/02724634.2011.550353

Antunes M. T. 1975. — *Iberosuchus*, crocodile Sebecosuchien nouveau, l'Eocène ibérique au nord de la Chaîne central, et l'origine du canyon de Nazare. *Comunicaçoes dos Servicos Geologicos de Portugal* 59: 285-330.

Antunes M. T. & Cahuzac B. 1999. — Crocodilian faunal renewal in the upper Oligocene of Western Europe. *Comptes rendus de l'Académie des Sciences Paris, Science de la terre et des planètes* 328: 67-73.

Berg D. E. 1966. — Die Krokodile, insbesondere *Asiatosuchus* and aff. *Sebecus*?, aus dem Eozan von Messel bei Darmstadt/Hessen. *Abhandlungen des Hessischen Landesamtes fur Bodenforschung* 52: 1-105.

Bremer K. 1994. — Branch support and tree stability. Cladistics 10: 295-304. https://doi.org/10.1111/j.1096-0031.1994.tb00179.x

Brochu C. A. 1999. — Phylogenetics, taxonomy, and historical biogeography of Alligatoroidea. *Journal of Vertebrate Paleontology* 19 (S2): 9-100. https://doi.org/10.1080/02724634.1999.10011201

Brochu C. A. 2000. — *Borealosuchus* (Crocodylia) from the Paleocene of Big Bend National Park, Texas. *Journal of Paleontology* 74: 181-187. https://doi.org/10.1017/S0022336000031358

Brochu C. A. 2001. — Congruence between physiology, phylogenetics and the fossil record on crocodylian historical biogeography, *in* Grigg G. C., Seebacher F. & Franklin C. E. (eds), *Crocodilian biology and evolution*. Surrey Betty & Sons, Chipping Norton NSW, Australia, 446 p.

Brochu C. A. 2004. — Alligatorine phylogeny and the status of *Allognathosuchus* Mook, 1921. *Journal of Vertebrate Paleontology* 24 (4): 857-873. https://doi.org/cxfpg8

Brochu C. A. 2007. — Systematics and taxonomy of Eocene tomistomine crocodylians from Britain and Northern Europe. *Palaeontology* 50 (4): 917-928. https://doi.org/10.1111/j.1475-4983.2007.00679.x

Brochu C. A. 2013. — Phylogenetic relationships of Palaeogene ziphodont eusuchians and the status of *Pristichampsus* Gervais, 1853. *Earth and Environmental Science Transactions of the Royal Society of Edinburgh* 103: 521-550. https://doi.org/10.1017/S1755691013000200

Brochu C. A. & Storrs G. W. 2012. — A giant crocodile from the Plio-Pleistocene of Kenya, the phylogenetic relationships of Neogene African crocodylines, and the antiquity of *Crocodylus* in Africa. *Journal of Vertebrate Paleontology* 32: 587-602. https://doi.org/10.1080/02724634.2012.652324

Buffetaut E. 1988. — The ziphodont mesosuchian crocodile from Messel: a reassessment. *Courier Forschungsinstitut Senckenberg* 107: 211-221.
Buscalioni A. D., Sanz J. L. & Casanovas M. L. 1992. — A new species of the eusuchian crocodile *Diplocynodon* from the Eocene of Spain. *Neues Jahrbuch für Geologie und Paläontologie Abhandlungen* 187: 1-29.
Čerňanský A., Tóth C. & Šurka J. 2012. — Crocodylian and turtle finds from the Lower Miocene of the Baňa Dolina mine in Veľký Krtíš (Slovakia). *Acta Geologica Slovaca* 4: 113-123.
Chroust M., Mazuch M. & Luján À. H. 2019. — New crocodilian material from the Eocene-Oligocene transition of the NW Bohemia (Czech Republic): an updated fossil record in Central Europe during the Grande Coupure. *Neues Jahrbuch für Geologie und Paläontologie Abhandlungen* 293: 73-82. https://doi.org/10.1127/njgpa/2019/0832
Codrea V., Vremir M. & Dica P. 1997. — Calcarul de Cluj de la Someş-Dig (Cluj-Napoca): semnificaţii paleoambientale şi impactul activităţilor antropice asupra aflorimentului. *Complexul Muzeal judeţean Bistriţa-Năsăud, Studii şi cercetări* 3: 31-39.
Codrea V. A. & Venczel M. 2020. — The fossil record of Palaeogene crocodilians of Romania: preliminary data. *Nymphaea* 46-47: 67-82.
Cossette A. P. & Brochu C. A. 2018. — A new specimen of the alligatoroid *Bottosaurus harlani* and the early history of character evolution in alligatorids. *Journal of Vertebrate Paleontology* 38: 1-22. https://doi.org/10.1080/02724634.2018.1486321
Delfino M., Piras P. & Smith T. 2005. — Anatomy and phylogeny of the gavialoid crocodylian *Eosuchus lerichei* from the Paleocene of Europe. *Acta Palaeontologica Polonica* 50 (3): 565-580.
Delfino M. & Smith T. 2009. — A reassessment of the morphology and taxonomic status of '*Crocodylus*' *depressifrons* Blainville, 1855 (Crocodylia, Crocodyloidea) based on the Early Eocene remains from Belgium. *Zoological Journal of the Linnean Society* 156: 140-167. https://doi.org/10.1111/j.1096-3642.2008.00478.x
Delfino M. & Smith T. 2012. — Reappraisal of the morphology and phylogenetic relationships of the middle Eocene alligatoroid *Diplocynodon deponiae* (Frey, Laemmert, and Riess, 1987) based on a three-dimensional specimen. *Journal of Vertebrate Paleontology* 32 (6): 1358-1369. https://doi.org/10.1080/02724634.2012.699484
Delfino M., Böhme M. & Rook. L. 2007. — First European evidence for transcontinental dispersal of *Crocodylus* (late Neogene of southern Italy). *Zoological Journal of Linnean Society* 149: 239-307. https://doi.org/10.1111/j.1096-3642.2007.00248.x
Delfino M., Martin J. E., de Lapparent de Broin F. & Smith T. 2017. — Evidence for a pre-PETM dispersal of the earliest European crocodyloids. *Historical Biology* 2017: 1-8.
Díaz Aráez J. L., Delfino M., Luján A. H., Fortuny J., Bernardini F. & Alba D. M. 2017. — New remains of *Diplocynodon* (Crocodylia: Diplocynodontidae) from the Early Miocene of the Iberian Peninsula. *Comptes Rendus Palevol* 16 (1): 12-26. https://doi.org/10.1016/j.crpv.2015.11.003
Diedrich C. G. 2013. — The most northerly record of the sirenian *Protosiren* and the possible polyphyletic evolution of manatees and dugongs. *Natural Sciences* 5 (11): 1154-1164. https://doi.org/10.4236/ns.2013.511142
Fărcaş C. 2011. — Studiul formaţiunilor continentale eocen terminale şi oligocen timpurii din NV-ul Depresiunii Transilvaniei – biostratigrafie şi reconstituiri ambientale, pe baza asociaţiilor de vertebrate continentale. Unpubl. PhD thesis, Babeş-Bolyai Univesity, Cluj-Napoca, 213 p.
Farkas B. 1995. — Fossil trionychid turtle types in Hungarian collections – preliminary review (Reptilia, Testudines). *Annales Historico-Naturales Musei Nationalis Hungarici* 87: 57-62.
Fărcaş C. & Codrea V. 2008. — Overview on the Eocene/Oligocene boundary formations bearing mammals in northwestern Transylvania. *Drobeta Seria Ştiinţele Naturii* 18: 24-32.
Gervais P. 1871. — Remarques au sujet des Reptiles provenant des calcaires lithographiques de Cerin, dans le Bugey, qui sont conserves au Musee de Lyon. *Comptes Rendus des seances de l'Academie de Sciences* 73: 603-607.
Godoy P. L., Benson R. B. J., Bronzati M. & Butler R. J. 2019. — The multi-peak adaptive landscape of crocodylomorph body size evolution. *BMC Evolutionary Biology* 19:167. https://doi.org/10.1186/s12862-019-1466-4
Goloboff P. A., Farris J. S. & Nixon K. C. 2008. — TNT, a free program for phylogenetic analysis. *Cladistics* 24: 774-786. https://doi.org/10.1111/j.1096-0031.2008.00217.x
Grigg G. & Kirshner D. 2015. — Biology and evolution of crocodylians. Cornell University Press, Ithaca, New York, 649 p.
Hastings A. K. & Hellmund M. 2015. — Rare in situ preservation of adult crocodylian with eggs from the middle Eocene of Geiseltal, Germany. *Palaios* 30: 446-461. https://doi.org/10.2110/palo.2014.062
Holliday C. & Witmer L. M. 2007. — Archosaur adductor chamber evolution: integration of musculoskeletal and topological criteria in jaw muscle homology. *Journal of Morphology* 268: 457-484. https://doi.org/10.1002/jmor.10524
Hurlburt G. R., Heckert A. B. & Farlow J. O. 2003. — Body mass estimates of phytosaurs (Archosauria: Parasuchidae) from the Petrified Forest Formation (Chinle group: Revueltian) based on skull and limb bone measurements, *in* Zeigler K. E., Heckert A. B. & Lucas S. G. (eds), Paleontology and Geology of the Snyder Quarry. *New Mexico Museum of Natural History and Science Bulletin* 24: 105-114.
Huxley T. H. 1875. — On *Stagonolepis robertsoni*, and the evolution of the Crocodilia. *Quarterly Journal of the Geological Society* 31: 423-431. https://doi.org/10.1144/GSL.JGS.1875.031.01-04.29
Koch A. 1894. — Az Erdélyrészi medencze harmadkori képződményei, I Paleogén csoport. *Földtani Intézet évkönyve* 10: 161-356.
Kuhn O. 1968. — *Die vorzeitlichen Krokodile*. Verlag Oeben, München, 124 p.
Li C., Wu X.-C. & Rufolo S. J. 2019. — A new crocodyloid (Eusuchia: Crocodylia) from the upper cretaceous of China. *Cretaceous Research* 94: 25-39. https://doi.org/10.1016/j.cretres.2018.09.015
Luján A. H., Chroust M., Čerňanský A., Fortuny J., Mazuch M. & Ivanov M. 2019. — First record of *Diplocynodon ratelii* Pomel, 1847 from the early Miocene site of Tušimice (Most Basin, Northwest Bohemia, Czech Republic). *Comptes Rendus Palevol* 18 (7): 877-889. https://doi.org/10.1016/j.crpv.2019.04.002
Macaluso L., Martin J. E., Del Favero L. & Delfino M. 2019. — Revision of the crocodilians from the Oligocene of Monteviale, Italy, and the diversity of European eusuchians across the Eocene-Oligocene boundary. *Journal of Vertebrate Paleontology* e1601098. https://doi.org/10.1080/02724634.2019.1601098
Martin J. E. 2010. — A new species of *Diplocynodon* (Crocodylia, Alligatoroidea) from the Late Eocene of the Massif Central, France, and the evolution of the genus in the climatic context of the Late Palaeogene. *Geological Magazine* 147: 596-610. https://doi.org/10.1017/S0016756809990161
Martin J. E. 2015. — A sebecosuchian in a middle Eocene karst with comments on the dorsal shield in Crocodylomorpha. *Acta Palaeontologica Polonica* 60 (3): 673-680.
Martin J. E. 2016. — New material of the ziphodont mesoeucrocodylian *Iberosuchus* from the Eocene of Languedoc, southern France. *Annales de Paléontologie* 102 (2): 135-144. https://doi.org/10.1016/j.annpal.2016.05.002
Martin J. E. & Gross M. 2011. — Taxonomic clarification of *Diplocynodon* Pomel, 1847 (Crocodilia) from the Miocene of Styria, Austria. *Neues Jahrbuch für Geologie und Paläontologie Abhandlungen* 261: 177-193. https://doi.org/10.1127/0077-7749/2011/0159
Martin J. E., Smith T., de Lapparent de Broin F., Escuillié F. & Delfino M. 2014. — Late Palaeocene eusuchian remains from Mont de Berru, France and the origin of the alligatoroid

Diplocynodon. *Zoological Journal of the Linnean Society* 172: 867-891. https://doi.org/10.1111/zoj.12195

MASSONE T., VASILYAN D., RABI M. & BÖHME M. 2019. — A new alligatoroid from the Eocene of Vietnam highlights an extinct Asian clade independent from extant *Alligator sinensis*. *PeerJ* 7: e7562. https://doi.org/10.7717/peerj.7562

MÉSZÁROS N. 2000. — Correlation of the Paleogene and Neogene deposits from Northern Transylvania. *Studia Universitatis Babeş-Bolyai, Geologia* 45 (2): 9-12. https://doi.org/10.5038/1937-8602.45.2.1

MLÍKOVSKÝ J. 2007. — Taxonomic identity of *Eostega lebedinskyi* Lambrecht, 1929 (Aves) from the middle Eocene of Romania. *Annalen des Naturhistorischen Museums in Wien* 109A: 19-27.

MONTEFELTRO F. C., ANDRADE D. V. & LARSSON H. C. E. 2016. — The evolution of the meatal chamber in crocodyliforms. *Journal of Anatomy* 228: 838-863. https://doi.org/10.1111/joa.12439

MOOK C. C. 1925. — A revision of the Mesozoic Crocodilia of North America (preliminary report). *Bulletin American Museum of Natural History* 51: 319-432.

ORTEGA F., BUSCALIONI A. D & GASPARINI Z. 1996. — Reinterpretation and new denomination of *Atacisaurus crassiproratus* (Middle Eocene; Issel, France) as cf. *Iberosuchus* (Crocodylomorpha, Metasuchia)". *Geobios* 29 (3): 353-364. https://doi.org/10.1016/S0016-6995(96)80037-4

ŐSI A. 2014. — The evolution of jaw mechanism and dental function in heterodont crocodyliforms. *Historical Biology*: 26 (3): 279-414. https://doi.org/10.1080/08912963.2013.777533

PICTET F. J. 1857. — Description des ossements fossiles trouvés au Mauremont, *in* PICTET F.-J., GAUDIN C. & DE LA HARPE P. (eds), *Mémoire sur les Animaux Vertébrés Trouvés dans le Terrain Sidérolithique du Canton de Vaud et Appartenant à la Faune Éocène, Volume 2, Matériaux de Paléontologie Suisse (note 1)*. Kessmann J., Geneva: 27-120.

PIRAS P. & BUSCALIONI A. D. 2006. — *Diplocynodon muelleri* comb. nov., an Oligocene diplocynodontine alligatoroid from Catalonia (Ebro Basin, Lleida Province, Spain). *Journal of Vertebrate Paleontology* 26 (3): 608-620. https://doi.org/fnjnhc

PIRAS P., DELFINO M., DEL FAVERO L. & KOTSAKIS T. 2007. — Phylogenetic position of the crocodylian *Megadontosuchus arduini* (de Zigno, 1880) and tomistomine palaeobiogeography. *Acta Palaeontologica Polonica* 52 (2): 315-328.

RAGE J.-C. & ROČEK Z. 2003. — Evolution of anuran assemblages in the Tertiary and Quaternary of Europe, in the context of palaeoclimate and palaeogeography. *Amphibia-Reptilia* 24: 133-167. https://doi.org/10.1163/156853803322390408

RIO J. P., MANNION P. D., TSCHOPP E., MARTIN J. E. & DELFINO M. 2020. — Reappraisal of the morphology and phylogenetic relationships of the alligatoroid crocodylian *Diplocynodon hantoniensis* from the late Eocene of the United Kingdom. *Zoological Journal of the Linnaean Society* 188: 579-629.

ROSSMANN T. 2000. — Skelettanatomische Beschreibung von *Pristichampsus rollinatii* (Gray) (Crocodilia, Eusuchia) aus dem Paläogen von Europa, Nordamerika und Ostasien. *Courier Forschungsinstitut Senckenberg* 221: 1-107.

ROSSMANN T. & BLUME M. 1999. — Die Krokodil-Fauna der Fossillagerstatte Grube Messel: ein aktueller Uberblick. *Natur und Museum* 129: 261-270.

SERRANO-MARTÍNEZ A., KNOLL F., NARVÁEZ I., ORTEGA F. 2019. — Brain and pneumatic cavities of the braincase of the basal alligatoroid *Diplocynodon tormis* (Eocene, Spain). *Journal of Vertebrate Paleontology* 39: 1, e1572612. https://doi.org/10.1080/02724634.2019.1572612

STEHLIN H. G. 1909. — Remarques sur les faunules de Mammifères des couches éocènes et oligocènes du bassin de Paris. *Bulletin de la Société géologique de France*, *4e série* (9): 488-520.

SUESS H. D. 2019. — The rise of reptiles: 320 million years of evolution. John Hopkins University Press, Baltimore, 400 p. https://doi.org/10.1353/book.67468

TAPLIN L. E. 1984. — Homeostasis of plasma electrolytes, sodium and water pools in the estuarine crocodile, *Crocodylus porosus*, from fresh, saline and hypersaline waters. *Oecologia* 63: 63-70. https://doi.org/10.1007/BF00379786

TAPLIN L. E. 1988. — Osmoregulation in crocodilians. *Biological Reviews of the Cambridge Philosophical Society* 63: 333-377. https://doi.org/10.1111/j.1469-185X.1988.tb00721.x

WANG Y. Y., SULLIVAN C. & LIU J. 2016. — Taxonomic revision of *Eoalligator* (Crocodylia, Brevirostres) and the paleogeographic origins of the Chinese alligatoroids. *PeerJ* 4 (5562): e2356. https://doi.org/10.7717/peerj.2356

WHEATLEY P. V. 2010 — Understanding salt water tolerance and marine resource use in the Crocodylia: a stable isotope approach. PhD thesis, University of California, Santa Cruz.

WHEATLEY P. V., PECKHAM H., NEWSOME S. D. & KOCH P. L. 2012. — Marine resource use in the American crocodile (*Crocodylus acutus*) in Southern Florida. *Marine Ecology Progress Series* 447: 211-229. https://doi.org/10.3354/meps09503

WU X.-C., BRINKMAN D. B. & FOX R. C. 2001. — A new crocodylian (Archosauria) from the basal Paleocene of the Red Deer River Valley, southern Alberta. *Canadian Journal of Earth Science* 38: 1689-1704.

Submitted on 27 October 2020;
accepted on 11 January 2021;
published on 17 May 2022.